



HAL
open science

GAPDH Expression Predicts the Response to R-CHOP, the Tumor Metabolic Status, and the Response of DLBCL Patients to Metabolic Inhibitors

Johanna Chiche, Julie Reverso-Meinietti, Annabelle Mouchotte, Camila Rubio-Patino, Rana Mhaidly, Elodie Villa, Jozef P. Bossowski, Emma Proics, Manuel Grima-Reyes, Agnes Paquet, et al.

► To cite this version:

Johanna Chiche, Julie Reverso-Meinietti, Annabelle Mouchotte, Camila Rubio-Patino, Rana Mhaidly, et al.. GAPDH Expression Predicts the Response to R-CHOP, the Tumor Metabolic Status, and the Response of DLBCL Patients to Metabolic Inhibitors. *CELL METABOLISM*, 2019, 29 (6), pp.1243+. 10.1016/j.cmet.2019.02.002 . hal-02359440

HAL Id: hal-02359440

<https://hal.science/hal-02359440>

Submitted on 25 Oct 2021

HAL is a multi-disciplinary open access archive for the deposit and dissemination of scientific research documents, whether they are published or not. The documents may come from teaching and research institutions in France or abroad, or from public or private research centers.

L'archive ouverte pluridisciplinaire **HAL**, est destinée au dépôt et à la diffusion de documents scientifiques de niveau recherche, publiés ou non, émanant des établissements d'enseignement et de recherche français ou étrangers, des laboratoires publics ou privés.



Distributed under a Creative Commons Attribution - NonCommercial 4.0 International License

1 **GAPDH expression predicts the response to R-CHOP, the tumor metabolic** 2 **status and the response of DLBCL patients to metabolic inhibitors**

3 Johanna Chiche¹, Julie Reverso-Meinietti^{1,2}, Annabelle Mouchotte¹, Camila Rubio-Patiño¹, Rana
4 Mhaidly¹, Elodie Villa¹, Jozef P. Bossowski¹, Emma Proics¹, Manuel Grima-Reyes¹, Agnès Paquet³,
5 Konstantina Fragaki^{4,5,6}, Sandrine Marchetti¹, Josette Briere⁷, Damien Ambrosetti², Jean-François
6 Michiels^{2,4}, Thierry Jo Molina⁸, Christiane Copie-Bergman⁹, Jacqueline Lehmann-Che¹⁰, Isabelle
7 Peyrottes¹¹, Frederic Peyrade¹¹, Eric De Kerviler¹², Bruno Taillan¹³, Georges Garnier¹³, Els
8 Verhoeyen¹, Véronique Paquis-Flucklinger^{4,5,6}, Laetitia Shintu¹⁴, Vincent Delwail¹⁵, Celine Delpech-
9 Debiais¹⁶, Richard Delarue¹⁷, André Bosly¹⁸, Tony Petrella¹⁹, Gabriel Brisou²⁰, Bertrand Nadel²⁰,
10 Pascal Barbry³, Nicolas Mounier²¹, Catherine Thieblemont^{7,22,*} and Jean-Ehrland Ricci^{1,23,*}

11 1: Université Côte d'Azur, INSERM, C3M, Nice, France.

12 2: Centre Hospitalier Universitaire de Nice, Département d'anatomo-pathologie, Nice, France,
13 Laboratoire Central d'Anatomocytologie (LCAP), CHU de Nice

14 3: Université Côte d'Azur, CNRS, Institut de Pharmacologie Moléculaire et Cellulaire, 06560 Sophia
15 Antipolis, France

16 4: Université Côte d'Azur, Nice, France

17 5: IRCAN, UMR CNRS 7284/INSERM U1081/UNS, School of Medicine, Nice Sophia-Antipolis
18 University, France

19 6: Department of Medical Genetics, National Centre for Mitochondrial Diseases, Nice Teaching
20 Hospital, France

21 7: APHP Hôpital Saint-Louis, Hémato-oncologie – Université Paris Diderot, Sorbonne Paris cité, Paris
22 France

23 8: Département de Pathologie, Hôpital Necker, AP-HP, EA 7324, Université Paris Descartes,
24 Sorbonne Paris Cité, Paris, France

25 9: IMRB-Inserm U955, AP-HP Hôpital Henri Mondor, Créteil, France.

26 10: AP-HP, Hôpital Saint Louis, Unité d'oncologie moléculaire, Univ Paris Diderot, Sorbonne Paris
27 Cité, 75010 Paris, France

28 11: Centre Antoine-Lacassagne, Nice, France

29 12: APHP, Hôpital Saint-Louis. Service de Radiologie, Université Paris Diderot, Sorbonne Paris Cité,
30 F-75010 Paris, France

31 13: Centre Hospitalier Princesse Grace de Monaco, Monaco

32 14: Aix Marseille Univ, CNRS, Centrale Marseille, Institut des Sciences Moléculaires de Marseille
33 (ISM2), Marseille, France

34 15: Service d'Oncologie Hématologique et de Thérapie Cellulaire, CHU de Poitiers, INSERM, CIC
35 1402, Centre d'Investigation Clinique, Université de Poitiers, France

36 16: Department of Pathology, CHU/Université de Poitiers, Poitiers, France

37 17: Department of Hematology, AP-HP Hôpital Necker, Paris, France.

38 18: CHU Dinant Godinne, UCL Namur, Yvoir, Belgium.

39 19: Department of Pathology, Hôpital Maisonneuve-Rosemont, Montréal, Quebec, Canada.

40 20 : Aix Marseille Univ, CNRS, INSERM, CIML, Marseille, France.

41 21: Centre Hospitalier Universitaire de Nice, Département d'Onco-Hématologie, Nice, France.

42 22: NF-kappaB, Différenciation et Cancer, EA7324, Université Paris Descartes, Paris France.

43 23 Lead contact : Jean-Ehrland Ricci, Ph.D.

44

45 *: Co-corresponding authors

46 • Jean-Ehrland Ricci, Ph.D, Inserm U1065, équipe 3, 151 route de Ginestière, BP 2 3194, 06204
47 Nice Cedex 03, France. Phone: +33 4 89 06 43 04; Fax +33 4 89 06 42 21, email:
48 ricci@unice.fr

49 • Catherine Thieblemont, M.D., Ph.D, AP-HP-Hôpital Saint-Louis, Service d'hémato-
50 Oncologie, Paris, email : catherine.thieblemont@sls.aphp.fr

51

52

1 **Summary**

2 Diffuse large B-cell lymphoma (DLBCL) is a heterogeneous disease treated with anti-CD20-based
3 immuno-chemotherapy (R-CHOP). We identified that low levels of GAPDH predict a poor response
4 to R-CHOP treatment. Importantly, we demonstrated that GAPDH^{low} lymphomas use OxPhos
5 metabolism and rely on mTORC1 signaling and glutaminolysis. Consistently, disruptors of OxPhos
6 metabolism (phenformin) or of glutaminolysis (L-asparaginase) induce cytotoxic responses in
7 GAPDH^{low} B cells and improve GAPDH^{low} B lymphoma-bearing mice survival, while they are low/no
8 efficient on GAPDH^{high} B lymphomas. Ultimately, we selected four GAPDH^{low} DLBCL patients, that
9 were refractory to all anti-CD20-based therapies and targeted DLBCL metabolism using L-
10 asparaginase (K), mTOR inhibitor (T) and metformin (M) (called KTM therapy). Three out of the four
11 patients presented a complete response upon one cycle of KTM. These findings establish that GAPDH
12 expression level predicts DLBCL patients' response to R-CHOP treatment and their sensitivity to
13 specific metabolic inhibitors.

14

15 **Keywords:** DLBCL, R-CHOP, metabolism, OxPhos, glycolysis, mTOR, predictive marker, L-
16 asparaginase

17

18

19

1 **Introduction**

2 Diffuse large B-cell lymphoma (DLBCL) is a genetically heterogeneous group of tumors and the most
3 common type of lymphoid malignancies (Swerdlow et al., 2016). DLBCLs represent highly
4 metabolically active tumors previously treated with a polychemotherapy CHOP (cyclophosphamide,
5 hydroxydaunorubicin, Oncovin® and prednisone) (Fisher et al., 1993). Since 1998, immunotherapy
6 anti-CD20 (Rituximab) combined with CHOP (referred as R-CHOP) became the standard treatment
7 for this disease, as it significantly improved the survival of patients (Coiffier et al., 2002). However,
8 approximately 40% of patients with DLBCL still experience therapeutic failure upon R-CHOP (Sehn
9 and Gascoyne, 2015). DLBCLs molecular heterogeneity is considered a major factor influencing the
10 response to R-CHOP therapy (Lenz and Staudt, 2010; Lenz et al., 2008). The cell-of-origin (COO)
11 classification delineates DLBCL subsets into distinct transcriptional profiles: the Germinal Center B-
12 cell (GCB)-, the Activated B-cell (ABC)- and the Unclassified-DLBCL subtypes (Alizadeh et al.,
13 2000). Unlike GCB-DLBCLs, ABC-DLBCLs are associated with a poor outcome upon R-CHOP
14 treatment (Lenz et al., 2008). Comparison of other gene signatures highlighted three other DLBCL
15 clusters that are recapitulated in the consensus cluster classification (CCC): i) the B cell receptor
16 (BCR)/proliferation (BCR-DLBCL) up-regulates genes encoding BCR signaling components; ii) the
17 oxidative phosphorylation (OxPhos) cluster (OxPhos-DLBCL) is enriched in genes involved in
18 electron transport chain (ETC) complexes, OxPhos metabolism and in other mitochondrial functions
19 and iii) the host response (HR) cluster is characterized by a host inflammatory infiltrate (Monti et al.,
20 2005). Importantly, there is no link between the COO and the CCC classifications (Caro et al., 2012;
21 Monti et al., 2005). Further characterization demonstrated that OxPhos-DLBCL cell lines lack the B
22 cell receptor and are insensitive to inhibition of the BCR signaling pathway (Chen et al., 2008). In
23 contrast, BCR-DLBCL cell lines express a functional BCR and primarily rely on glycolysis to produce
24 energy (Caro et al., 2012; Chen et al., 2008). Altogether those studies have identified, for the first
25 time, the metabolic heterogeneity within the same tumor entity (Caro et al., 2012; Monti et al., 2005;
26 Norberg et al., 2017). However, whether distinct metabolic fingerprints influence DLBCL response to
27 R-CHOP remains unknown. Moreover, it is unclear whether targeting DLBCL metabolic specificity

1 might be a valuable therapeutic approach in the clinic, in particular for R-CHOP low responder
2 patients. In this study, we addressed two unmet clinical needs: can we identify, at the diagnosis, which
3 DLBCL patients is likely to be a low responder to R-CHOP? and can we foretell if those patients will
4 be likely to respond to specific metabolic inhibitors according to their DLBCL's metabolic status?
5 Using unbiased analysis, we identified the glyceraldehyde-3-phosphate dehydrogenase, GAPDH, as
6 the only glycolytic enzyme able to predict overall survival of patients with DLBCL treated with R-
7 CHOP. Moreover, we established *in vivo* as well as in the clinic, that GAPDH holds potential as a
8 marker of DLBCL metabolic status and of patients's response to specific metabolic inhibitors.

9

10 **Results**

11

12 **GAPDH expression predicts overall survival of patients with DLBCL treated with R-CHOP and** 13 **DLBCL metabolic status.**

14 Unbiased analysis of expression profile data set from 233 newly diagnosed DLBCLs (Lenz et al.,
15 2008) allowed us to identify 587 probesets ($p < 0.05$), corresponding to 524 unique genes associated
16 with differences in overall survival (OS) upon R-CHOP treatment (Table S1, Fig S1A). Analysis of
17 molecular functions associated with OS predicting genes, identified classical pathways involved in
18 resistance to chemotherapies (cell survival, proliferation, DNA repair...) and highlighted the
19 mitochondrial energetic function (Table S1 and Fig S1B). In contrast, only one gene involved in
20 glycolysis, the glyceraldehyde-3-phosphate dehydrogenase (*gapdh*) predicts a favorable outcome
21 when highly expressed (3 independent probesets: HR= 0.53, 0.53 and 0.54 and corresponding p
22 value= 0.01573, 0.01771 and 0.01929; Table S1). Of note, we also observed that lactate
23 dehydrogenase b subunit (*ldhb*) is significantly associated with a poor outcome (Table S1). Though,
24 LDH-B converts lactate to pyruvate, a source for OxPhos metabolism or for gluconeogenesis (Doherty
25 and Cleveland, 2013), we focused our attention on *gapdh*.

26

1 When subgrouping DLBCLs according to *gapdh* mRNA levels (high or low, Fig 1A), patients with
2 DLBCL-*gapdh*^{low} have a lower OS upon R-CHOP than those with DLBCL-*gapdh*^{high} (Fig 1B). To
3 further determine whether GAPDH protein expression predicts differences in OS upon R-CHOP, we
4 set up an automated immuno-histochemical (IHC) staining of GAPDH and a scoring system to
5 quantify its expression in 43 newly diagnosed DLBCL (training cohort, Table S2). As for *gapdh*
6 mRNA (Fig 1B), DLBCLs expressing low levels of GAPDH protein (GAPDH^{low}, score ≤ 150) are
7 associated with a poorer OS upon R-CHOP than DLBCLs expressing high levels of GAPDH
8 (GAPDH^{high}, score > 150) (Figs 1D and 1E, see also STAR methods for determination of GAPDH
9 IHC score and cutoff of 150). This finding was confirmed in a larger cohort of 294 *de novo* DLBCLs
10 treated with R-CHOP (validation cohort, Table S2) (Delarue et al., 2013) by staining and scoring
11 GAPDH from paraffin-embedded tissue microarray (TMA) using the previously established IHC score
12 cutoff (Figs 1F and 1G).

13 Interestingly, GAPDH expression is not associated with clinical factors such as age-adjusted
14 International Prognostic Index (aaPI), COO or Hans classification (Hans et al., 2004), expression of
15 bad prognosis markers, double hit (*MYC/BCL2*) or triple hit (*MYC/BCL2/BCL6*) translocations
16 previously validated in DLBCLs (Horn et al., 2013; Johnson et al., 2012) (Table 1). Of note, there is
17 no difference in OS noted on the basis of BCL6, or MYC or MYC-BCL2 expressions in the validation
18 cohort. However, BCL2 expression significantly impacts the OS (Petrella et al., 2017). Multivariate
19 analysis showed that GAPDH^{high} expression remained a significant marker predicting improved OS
20 (HR=0.603, p=0.0371), independently of BCL2 (HR=1.686, p=0.0213). When compared to the aaPI,
21 multivariate analysis showed that GAPDH expression also remained a significant marker predicting
22 improved OS in the training and validation cohorts (Table S3).

23 Altogether, these results demonstrate that the predictive value of GAPDH expression levels is
24 independent of known biomarkers/factors of poor prognosis.

25

26 According to the CCC classification, we observed that 69% of DLBCL-*gapdh*^{low} (n=49/71) are
27 OxPhos-DLBCLs, while 61% of DLBCL-*gapdh*^{high} (n=51/82) belong to the BCR/proliferation cluster

1 associated with glycolysis (two-sided $p=0.00019$; analysis from (Lenz et al., 2008) cohort). OxPhos-
2 DLBCLs significantly express lower levels of *gapdh* mRNA than BCR-DLBCLs (Fig 1H). In
3 addition, we did not observe association between GAPDH expression levels and specific COO
4 subtypes in the training and validation cohorts (Table S2), consistent with the absence of correlation
5 between the CCC and the COO classification (Caro et al., 2012; Monti et al., 2005). Moreover,
6 patients with BCR- or OxPhos-DLBCL display the same outcome upon CHOP treatment (Monti et al.,
7 2005). Accordingly, distinct *gapdh* mRNA levels display similar OS when DLBCL are treated with
8 the polychemotherapy CHOP only (Fig S1C).

9 Arguments from the literature suggest that OxPhos-DLBCL- might be less sensitive than BCR-
10 DLBCL to Rituximab due to the lack of Syk (Spleen Tyrosine Kinase)-dependent BCR signaling
11 (Kheirallah et al., 2010). Compared to BCR-DLBCL cell lines (SU-DHL-4 and SU-DHL-6), i.e
12 glycolytic lymphoma cells expressing a functional BCR (IgM or IgG) (Chen et al., 2008), OxPhos-
13 DLBCL cell lines (Toledo and Karpas 422) express lower levels of GAPDH, secrete less lactate,
14 express neither IgM nor IgG and are less sensitive to Rituximab-induced death (Figs S2A to S2D). Of
15 note, GAPDH expression (mRNA and protein) is not influenced upon BCR activation with anti-IgM
16 in SU-DHL-6 (Fig S2E to S2G). In another approach, we investigated the energetic metabolic status of
17 malignant B cells harvested from fresh micro-biopsies of primary DLBCL tumors, according to the
18 level of GAPDH. DLBCL-GAPDH^{low} cells produce less glycolytic ATP than DLBCL-GAPDH^{high}
19 cells and there is a significant correlation between GAPDH expression level, and the percentage ATP
20 generated from glycolysis (Fig 1I).

21 We concluded that DLBCL-GAPDH^{low} are low responders to R-CHOP treatment and mainly rely on
22 OxPhos metabolism to fulfill their energetic demand.

23

24 **Mouse primary B lymphomas expressing low levels of GAPDH are sensitive to the inhibition of**
25 **mitochondrial ETC complex I.**

1 Identification of a novel biomarker predicting DLBCL sensitivity to current treatment is only of
2 clinical interest if we can propose new therapeutic options. Since R-CHOP low responders, i.e.
3 DLBCL-GAPDH^{low}, primarily rely on OxPhos metabolism (Fig 1H, 1I), we investigated their
4 sensitivity to inhibitors of mitochondrial energetics.

5 Using the pre-clinical E μ -Myc mouse model that spontaneously develop Non-Hodgkin (NH) B-cell
6 lymphomas (Adams et al., 1985), we wondered whether GAPDH expression levels could influence the
7 metabolic status of B lymphomas and the response to disruptors of mitochondrial metabolism *in vitro*
8 and *in vivo*. We previously characterized the expression of GAPDH in E μ -Myc lymphomas and
9 classified them according to the level of GAPDH (mRNA and protein) (GAPDH^{low} or GAPDH^{high}),
10 while the expression of the other glycolytic enzymes is similar between the two groups ((Chiche et al.,
11 2015) and Figs S3A to S3C). Of note, we did not observe any link between GAPDH and LDH (total or
12 LDH-B) expression (Fig S3A). While the exact nature of GAPDH regulation remains to be found,
13 *gapdh* mRNA was more stable in GAPDH^{high} than in GAPDH^{low} cells (Fig S3D). Cells from E μ -Myc-
14 GAPDH^{low} and E μ -Myc-GAPDH^{high} lymphomas produce equivalent amount of ATP (Fig 2A).
15 However, E μ -Myc-GAPDH^{low} cells produce less glycolytic ATP (Fig 2B), as observed in human
16 DLBCL cells (Fig 1H and 1I) and secrete less lactate than E μ -Myc-GAPDH^{high} cells (Fig 2C).
17 Accordingly, E μ -Myc-GAPDH^{low} cells consume more O₂ (Fig 2D), while glucose transporters
18 expression (Fig S3E) and the mitochondrial mass (Fig S3F) are similar between the two groups.

19 *In vitro*, the mitochondrial complex I inhibitor, phenformin (Wheaton et al., 2014) reduces baseline O₂
20 consumption driven by complex I and induces cytotoxic responses in E μ -Myc-GAPDH^{low} cells but not
21 in E μ -Myc-GAPDH^{high} cells (Figs 2E and S3G to S3I). Importantly, *gapdh*-silencing in E μ -Myc-
22 GAPDH^{high} cells decreases lactate production and increases cell sensitivity to phenformin-induced
23 death (Figs S4A to S4D). *In vivo*, phenformin treatment increases the survival of E μ -Myc-GAPDH^{low}
24 lymphoma-bearing mice, but not that of E μ -Myc-GAPDH^{high} lymphoma-bearing mice (Figs 2 F and
25 2G), which demonstrates the causal correlation between low expression of GAPDH and phenformin
26 sensitivity. We confirmed that phenformin was indeed active at the dose administrated *in vivo* (Figs
27 S3J-and S3K).

1 Overall, E μ -Myc-GAPDH^{low} lymphomas are sensitive to the inhibition of mitochondrial metabolism,
2 which represents a potential therapeutic strategy for patients with DLBCL-GAPDH^{low} that are low
3 responders to R-CHOP treatment.

4

5 **Active mTORC1 signaling in GAPDH low lymphomas is implicated in OxPhos metabolism.**

6 GAPDH was shown to modulate mTOR signaling through its binding to Rheb (Lee et al., 2009). We
7 therefore speculated that mTORC1 could be active in GAPDH^{low} B lymphomas. Indeed, we observed
8 a high mTORC1 activity in E μ -Myc-GAPDH^{low} lymphomas, as shown by p70-S6K phosphorylation
9 on threonine 389 (Fig 3A). This was confirmed in human DLBCL biopsies, for which 57% of
10 DLBCL-GAPDH^{low} stained positive for p70-S6K phosphorylation (indicating high mTORC1 activity),
11 while 91% of DLBCL-GAPDH^{high} do not express this form (indicating low mTORC1 activity) (Fig
12 3B).

13 Inhibition of mTORC1 signaling with rapamycin in E μ -Myc-GAPDH^{low} cells, decreases basal O₂
14 consumption rate, maximal respiratory capacities and ATP-coupled OCR along with an increase in
15 glycolytic ATP (Figs 3 C to 3G). Of note, the total amount of intracellular ATP was not modulated
16 upon rapamycin treatment (Fig S5A). More specifically, rapamycin decreases O₂ consumption driven
17 by complex I but not complex II (Figs S5B and S5C), due to the inhibition of complex I activity but
18 not of complex II activity (Fig S5D). The exact reason of such effect remains to be determined.
19 Similar results were obtained using an independent E μ -Myc-GAPDH^{low} lymphoma (Figs S5E to S5G).
20 As previously reported in several cancer cell lines (Fruman and Rommel, 2014), rapamycin does not
21 induce cytotoxic responses (Fig 3H), but rather cytostatic effects, as we observed (Fig S5H). Finally,
22 *in vivo* inhibition of mTORC1 activity with Temsirolimus (Dancey, 2010) significantly increases the
23 survival of OxPhos E μ -Myc-GAPDH^{low}-bearing mice (Figs 3I and 3J).

24 These results suggest that mTORC1 signaling is involved in the control of GAPDH^{low} B lymphoma
25 metabolism.

26

1 **B lymphomas expressing low levels of GAPDH rely on glutamine metabolism and are sensitive**
2 **to the hydrolysis of extracellular glutamine and asparagine with *E-Coli* L-asparaginase.**

3 mTORC1 is a central sensor of amino acids, including Gln (Duran et al., 2012). E μ -Myc-GAPDH^{low}
4 lymphomas display active mTORC1 signaling (Fig 3A) and consume more Gln than the E μ -Myc-
5 GAPDH^{high} cells (Fig 4A) due to a specific increase in Gln transport rates (Figs 4B, S6A and S6B).
6 We next profiled metabolic differences between E μ -Myc-GAPDH^{low} and E μ -Myc-GAPDH^{high}
7 lymphoma cells using liquid chromatography–mass spectrometry (LC-MS)–based metabolomics with
8 the intent to further characterize the intracellular fate of Gln (Fig 4C). The relative intracellular levels
9 of metabolites involved in glycolysis (G6P, G3P, lactate) and in the non-oxidative arm of the pentose
10 phosphate pathway (PPP) (Sedoheptulose-7-phosphate) are significantly decreased in E μ -Myc-
11 GAPDH^{low} cells (Fig 4C). Glutamine is metabolized through glutaminolysis to produce glutamate, α -
12 ketoglutarate, the latter being used to replenish the TCA cycle. In favor of an active glutaminolysis,
13 glutamate and α -ketoglutarate levels are higher in E μ -Myc-GAPDH^{low} cells (Fig 4C), consistent with
14 an increase expression of the glutaminase (GLS), the mitochondrial enzyme catalyzing the conversion
15 of glutamine into glutamate and ammonia (Fig 4D). While fewer metabolites could be detected by ¹H
16 HRMAS NMR spectroscopy, a significant increase in intracellular glutamate levels was also
17 confirmed in E μ -Myc-GAPDH^{low} cells (Figs S6C and S6D). Extracellular sources of Gln are required
18 for E μ -Myc-GAPDH^{low} cells to sustain basal O₂ consumption, maximal respiratory capacities and
19 ATP-coupled OCR (Figs S6E to S6G). Pharmacologic hydrolysis of extracellular sources of L-
20 glutamine and L-asparagine with *E-Coli* L-asparaginase (Fig 4E), reduces mTORC1 activity (Fig
21 S6H, (Willems et al., 2013)) and induces cytotoxic responses in E μ -Myc-GAPDH^{low} lymphoma cells
22 (Fig 4F). In addition, *gapdh*-silenced E μ -Myc-GAPDH^{high} lymphoma cells are more sensitive than
23 control cells to *E-Coli* L-ase-induced death (Fig S4E). *In vivo*, plasma sources of Gln were depleted in
24 *E-Coli* L-ase treated mice, regardless of the E μ -Myc lymphoma injected (Fig 4G). However, only the
25 survival of E μ -Myc-GAPDH^{low}-bearing mice was enhanced upon *E-Coli* L-ase treatment (Figs 4H and
26 4I). Of note, *E-Coli* L-ase treatment inhibited mTORC1 signaling *in vivo* (Figs S6I and S6J).

27

1 **Specific overexpression of GAPDH reduces mTORC1 signaling and B lymphomas sensitivity to**
2 **phenformin and L-asparaginase *in vivo*.**

3 To further support our conclusions, we overexpressed GAPDH in Eμ-*Myc*-GAPDH^{low} cells (Fig 5A).
4 GAPDH overexpression was sufficient to reduce mTORC1 signaling (Fig 5A) and to induce a
5 metabolic switch toward glycolysis, as judged by the increase in glycolytic ATP, lactate secretion
6 along with the reduction in baseline OCR and Gln consumption (Figs 5B to 5F). Equivalent
7 observations were obtained upon GAPDH expression in the OxPhos-DLBCL cell line Karpas 422
8 (Figs S7A to S7C). Importantly, the metabolic switch induced by GAPDH overexpression prevented
9 most of the beneficial effects brought by either phenformin or *E-Coli* L-asparaginase *in vivo* (Figs 5G
10 to 5I).

11 Together we confirmed that GAPDH expression influences the metabolic state and the sensitivity of B
12 lymphomas to phenformin or *E-Coli* L-asparaginase.

13

14 **Treatment of DLBCL-GAPDH^{low} with specific metabolic inhibitors demonstrates a significant**
15 **benefit for patients.**

16 We demonstrated that GAPDH^{low} B lymphomas preferentially use OxPhos metabolism to produce
17 energy and are sensitive to cell death induced by phenformin or *E-Coli* L-asparaginase. To ultimately
18 validate our findings, we designed a clinical therapeutic intervention (called KTM), to interfere with
19 DLBCL-GAPDH^{low} metabolism (Fig 6A). KTM therapy consists in 4 weeks-cycles of treatment
20 including *E-Coli* L-asparaginase (K, Kidrolase), mTOR inhibitor Temsirolimus (T, Torisel) and
21 Metformin (Fig 6B). The first two weeks, patients receive *E-Coli* L-asparaginase on days 1, 3, 5, 7, 9,
22 11, 13 and Temsirolimus on days 1, 7 and 14. This combination was not administered longer than 14
23 days since *E-Coli* L-asparaginase is not well tolerated in adults (Boissel and Sender, 2015). Instead,
24 the last two weeks of each KTM cycle, patients received metformin to sustain a therapeutic pressure
25 on mitochondrial metabolism (Fig 6B). It is important to consider that prior to KTM, patients were
26 refractory to all R-based therapies and only supportive care was proposed.

1 Fig 6C illustrates the patient#1, a 24-year-old man who presented a DLBCL in therapeutic failure. At
2 diagnosis, clinical presentation was a cervical bulky mass corresponding to a *Myc*-translocated GC-
3 DLBCL (diameter 240 x 100 mm) with bone marrow and blood infiltration (Table S4). Following
4 diagnosis, the patient received four regimens of immuno-chemotherapy. Early tumor progression was
5 systematically observed before initiating each new cycle of Rituximab-based therapy. Verification of
6 GAPDH expression at diagnosis by IHC showed a low GAPDH IHC score (of 35). As we could not
7 offer any other standard therapeutic option, patient #1 was selected for KTM treatment. 7 and 15 days
8 after the beginning of KTM therapy, the tumor mass significantly decreased (Fig 6C). After 30 days of
9 KTM treatment, patient #1 had 83% reduction of the tumor mass (Fig 6D) and was negative at PET-
10 Scan analysis. He had a normal life for 4 months and then died upon local and central nervous system
11 relapse of the lymphoma. To demonstrate that KTM efficacy is not limited to one single patient
12 presenting a DLBCL-GAPDH^{low}, three other patients with identical eligible criteria (*Myc*⁺-DLBCL-
13 GAPDH^{low} at diagnosis and treatments-refractory disease) were treated with KTM (Fig 6E). Three out
14 of four patients had a complete response after two cycles of treatment, and one patient had a
15 progressive disease due to early adverse events during the first cycle of treatment and KTM treatment
16 had to be discontinued (Fig 6F). Median duration of response was 6 months (4-6 mo).

17

18 **Discussion:**

19 Several metabolic inhibitors were developed with the intent to kill or to sensitize cancer cells to
20 chemotherapies (Galluzzi et al., 2013). So far, more than 100 clinical trials using metabolic inhibitors
21 are ongoing in the field of cancer (Meynet and Ricci, 2014). Unfortunately, to date, most of those
22 trials have failed to improve the outcome of patients (Kordes et al., 2015). This may not be linked to
23 the inefficacy of the compound to inhibit its target but rather to a subset of tumors with a distinct
24 metabolic dependence from the targeted metabolic pathway. Altogether, our study highlighted that
25 tumor heterogeneity within the same tumor entity has to be taken into consideration for ongoing
26 clinical trials using metabolic inhibitors.

1 While, more than 150'000 claimed biomarkers have been described in the literature, less than 100 are
2 routinely used in the clinic (Poste, 2011) and we still lack a marker of the tumor metabolic status.
3 Here, we identified GAPDH, as a clinically compatible biomarker of i) the conventional R-CHOP
4 treatment and of ii) the metabolic status of DLBCLs, which help to further predict the efficacy of
5 mitochondrial metabolism disruptors in the context of DLBCL-GAPDH^{low} that are associated with a
6 poor outcome of patients treated with R-CHOP.

7
8 GAPDH is a multifunctional protein harboring glycolytic and non-glycolytic functions (Colell et al.,
9 2009). It is highly regulated at the transcriptional, translational and post-translational levels.
10 Endogenous *gapdh* mRNA and protein are highly abundant in all mammalian cells and increased
11 expression levels of *gapdh* by 30% or more, significantly impacts on cell survival and growth (Colell
12 et al., 2009), particularly in B lymphomas (Chiche et al., 2015). We observed that human DLBCL
13 expressed heterogeneous levels of *gapdh* mRNA and protein defining patients with DLBCL-
14 GAPDH^{low} or DLBCL-GAPDH^{high}. As expected, when comparing healthy tissues (GCB cells from
15 non-cancerous reactive lymph nodes) to cancer samples, DLBCL-GAPDH^{low} express significantly
16 higher levels of GAPDH (Fig 1D). Moreover, when compared to DLBCL-GAPDH^{low}, DLBCL-
17 GAPDH^{high} express approximatively two times more GAPDH, which also highlights GAPDH as a
18 marker of tumor heterogeneity within the same tumor entity. Interestingly, *gapdh* mRNA stability was
19 higher in Eμ-*Myc*-GAPDH^{high} cells (Fig S3D). As GAPDH is an RNA binding protein (Colell et al.,
20 2009), we could speculate that it could bind and stabilize its own mRNA. However, the exact nature of
21 *gapdh* regulation in DLBCL is still unclear and will be investigated in further studies.

22
23 Mechanistically, we observed a central role of GAPDH-dependent regulation of mTORC1 signaling in
24 the control of DLBCL metabolic status. It was previously reported that *gapdh*-silenced HEK293 cells
25 increase mTORC1 signaling by preventing GAPDH-Rheb binding (Lee et al., 2009). Using the Eμ-
26 *Myc* model and newly diagnosed DLBCL samples we also observed an increase in mTORC1
27 signaling, glutamine uptake, glutaminolysis and sensitivity to L-asparaginase-induced death in

1 GAPDH^{low} B lymphomas (Fig 3 and 4). Altogether our findings are consistent with the role of
2 functional mTORC1 on glutamine uptake (Csibi et al., 2014) and the feedback role of glutaminolysis
3 on the activation of Rag-mTORC1 signaling (Duran et al., 2012). How GAPDH-dependent control of
4 mTORC1 regulates metabolism? mTORC1 is a known-regulator of HIF-1 α and c-Myc translation,
5 which in turn induce the expression of genes involved in glucose uptake and glycolysis (Gordan et al.,
6 2007). In primary E μ -Myc lymphomas, we did not observe differences in glucose transporters
7 expression (Fig S3E) according to GAPDH expression levels, despite differences in mTORC1
8 signaling. In contrast, inhibition of mTORC1 reduces O₂ consumption of E μ -Myc GAPDH^{low} cells, in
9 agreement with previous studies (Cunningham et al., 2007; Morita et al., 2013). It seems therefore
10 possible that E μ -Myc lymphomas and human DLBCLs do not follow the classical Warburg scheme in
11 which mTORC1 activates glycolysis. Instead, mTORC1 seems implicated in the regulation of OxPhos
12 metabolism in this biological model (Fig 3). This notion is further supported by the increase in
13 glutamine uptake, along with an increase in the relative intracellular levels of glutamate and α -
14 ketoglutarate and L-asparaginase efficacy on reduced mTORC1 signaling *in vitro* and *in vivo*
15 (Willems et al., 2013) (Figs 4 and S6).

16

17 Since IHC detection of GAPDH seemed to help for the determination of the tumor metabolic status,
18 we selected four patients with Myc⁺-DLBCL-GAPDH^{low}. All patients were refractory to R-based
19 therapies. In the face of a therapeutic dead end, we ultimately target DLBCLs-GAPDH^{low} metabolism
20 with already available (FDA-approved) metabolic disruptors (KTM therapy) (Fig 6). Based on the
21 observed cytostatic effect of Temsirolimus *in vitro* and *in vivo* (Figs 3I and S5H), we decided still to
22 administer this mTOR inhibitor either with L-asparaginase (D1, D7 of a KTR cycle) or with
23 Metformin (D14 of a KTR cycle) to maximize the potential beneficial effect of the co-treatment.
24 However, knowing that rapalogs alone or in combination with R-CHOP did not provide significant
25 benefits in randomized phase II and phase III trials for patients with NH B-cell lymphomas (Ricci and
26 Chiche, 2018), it is unlikely that the rapid and complete responses obtained after one week of KTM
27 treatment can be attributed to Temsirolimus. According to the beneficial effect observed in E μ -Myc-

1 GAPDH^{low} lymphomas upon *E-Coli* L-ase (Kidrolase) and to the early reduction of the tumor burden
2 observed from D7 in patient #1 (Fig 6C), it is likely that most of the treatment efficacy can be
3 attributed to the L-ase activity. Unfortunately, in the clinic, *E-Coli* L-ase cannot be administrated
4 longer than two weeks in a row in adults, as it may provoke major toxicities (Boissel and Sender,
5 2015). We therefore sustained inhibition of mitochondrial energetics with metformin and mTOR
6 inhibitor for the last two weeks of KTM cycle of treatment (Fig 6B). Despite the drastic reduction of
7 the tumor mass, all patients finally relapsed, which very likely reflect the metabolic flexibility and
8 adaptation of the remaining malignant B cells during or after KTM therapy.

9

10 **Limitations of study**

11 A major limitation in the field of DLBCL is a lack of robust pre-clinical models (cell lines or *in vivo*
12 mouse models) that recapitulate the major aspects of the human disease. As human cancer cell lines
13 were isolated decades ago and since grown in high glucose, high oxygen media, it is possible that their
14 metabolism do not reflect the metabolic status of the initial tumor cells. We therefore decided to
15 characterize several independent murine primary NH B cell lymphomas harvested from the E μ -Myc
16 mice model (Figs 2 to 5). While this model represents highly aggressive tumors (Ki67 100%) and is
17 largely used as a robust model to test new therapeutic options for NH B lymphomas, they lack key
18 features of human DLBCL such as marker of mature B cells. We therefore validated our findings in
19 humans, using malignant B cells immediately isolated from “fresh” DLBCL micro-biopsies and
20 ultimately by treating a few patients suffering from refractory disease with specific metabolic
21 inhibitors (Figs 1, 3 and 6). Another limitation of our work is the low number of patients included in
22 the KTM therapy. However, our study established the *proof-of-principle* that patients with DLBCL-
23 GAPDH^{low} are low responders to immuno-chemotherapy R-CHOP but are potential candidates for
24 KTM therapy. Finally, while GAPDH levels represent the first clinically compatible marker of
25 DLBCL metabolic heterogeneity, it remains to be determined if this marker can be extended to other
26 hematological malignances and to solid tumors.

27

1

2 **Acknowledgements**

3 We gratefully acknowledge the C3M animal facility, the Tumorothèque of Hôpital Saint-Louis and the
4 Lymphoma Study Association (LYSA). We thank the technician of the Laboratoire Central
5 d'Anatomocytologie (LCAP), CHU de Nice, S. Destrée and A. Borderie. We thank I.
6 Nemazany from the Platform for Metabolic Analyses (Neckert-Enfants Malades Institute, Paris). We
7 thank A. Vandenberghe, N. Alet, N. Jourdan-Desrayaud, F. Larbret, F. Reinier, N. Nottet, M. Baia, N.
8 Vailhen, S. Roulland, M. Zala, and I. Ben-Sahra for reagents and input. This work has been supported
9 by the Fondation ARC pour la Recherche sur le Cancer (PGA1 RC-20170205463), the Agence
10 Nationale de la Recherche (LABEX SIGNALIFE ANR-11-LABX-0028-01), the Fondation de France,
11 Centre Scientifique de Monaco, the Cancéropôle PACA and INSERM transfert. This project has
12 received funding from the European Union's Horizon 2020 research and innovation program under the
13 Marie Skłodowska-Curie grant agreement No 766214 (Meta-Can). C.T. is funded by the Nella and
14 Amadeus Barletta foundation (FNAB). BN is funded by Cancéropole PACA, la Fondation ARC
15 (PGA120150202381) and Plan cancer 2015 ITMO cancer (C15077AS). The IPMC functional
16 genomics platform is a member of the "France Génomique" consortium (ANR-10-Infra-01), with
17 financial support from the Cancéropôle PACA. E.Vil. is supported by La Ligue contre le Cancer; J.C.
18 is supported by foundation Tourette and France Lymphoma Espoir, G.B is supported by la Fondation
19 pour la Recherche Médicale (FRM, FDM20150734500) and J R-M. is supported by INCa.

20

21 **Author Contributions**

22 JC performed the majority of research described herein and was assisted by AM, C R-P, R M, E Vil.,
23 JPB, EP, MGR, KF, SM, E Ver., V P-F, LS, GB, BN. Clinical study and patient samples: J R-M, JB,
24 DA, J-FM, TJM, CC-B, JL-C, IP, FP, EDK, BT, GG, VD, CD-D, RD, AB, TP, NM, CT.
25 Bioinformatic analysis: AP, PB. J-E.R secured funding and supervised the study. CT supervised the
26 clinical study. JC and J-E.R designed research and wrote the manuscript.

1
2
3
4
5
6
7
8
9
10
11
12
13
14
15
16
17
18
19
20
21
22
23
24
25
26
27
28
29
30
31
32
33
34

Declaration of Interests,

CT is on the scientific board for Jazz Pharmaceuticals; Celgene; Roche, AbbVie; and Gilead.
The remaining authors declare no conflicts of interest.

Related patents:

WO2015/132163: A METHOD FOR PREDICTING THE RESPONSIVENESS A PATIENT TO A
TREATMENT WITH AN ANTI-CD20 ANTIBODY

WO2017/055484: METHODS FOR DETERMINING THE METABOLIC STATUS OF
LYMPHOMAS

EP17305294.5: A METHOD FOR PREDICTING THE RESPONSIVENESS OF A PATIENT TO A
TREATMENT WITH mTOR INHIBITORS

References

Adams, J.M., Harris, A.W., Pinkert, C.A., Corcoran, L.M., Alexander, W.S., Cory, S., Palmiter, R.D., and Brinster, R.L. (1985). The c-myc oncogene driven by immunoglobulin enhancers induces lymphoid malignancy in transgenic mice. *Nature* 318, 533-538.

Alizadeh, A.A., Eisen, M.B., Davis, R.E., Ma, C., Lossos, I.S., Rosenwald, A., Boldrick, J.C., Sabet, H., Tran, T., Yu, X., et al. (2000). Distinct types of diffuse large B-cell lymphoma identified by gene expression profiling. *Nature* 403, 503-511.

Boissel, N., and Sender, L.S. (2015). Best Practices in Adolescent and Young Adult Patients with Acute Lymphoblastic Leukemia: A Focus on Asparaginase. *J Adolesc Young Adult Oncol* 4, 118-128.

Caro, P., Kishan, A.U., Norberg, E., Stanley, I.A., Chapuy, B., Ficarro, S.B., Polak, K., Tondera, D., Gounarides, J., Yin, H., et al. (2012). Metabolic signatures uncover distinct targets in molecular subsets of diffuse large B cell lymphoma. *Cancer Cell* 22, 547-560.

Chen, L., Monti, S., Juszczynski, P., Daley, J., Chen, W., Witzig, T.E., Habermann, T.M., Kutok, J.L., and Shipp, M.A. (2008). SYK-dependent tonic B-cell receptor signaling is a rational treatment target in diffuse large B-cell lymphoma. *Blood* 111, 2230-2237.

Chiche, J., Pommier, S., Beneteau, M., Mondragon, L., Meynet, O., Zunino, B., Mouchotte, A., Verhoeyen, E., Guyot, M., Pages, G., et al. (2015). GAPDH enhances the aggressiveness and the vascularization of non-Hodgkin's B lymphomas via NF-kappaB-dependent induction of HIF-1alpha. *Leukemia* 29, 1163-1176.

Coiffier, B., Lepage, E., Briere, J., Herbrecht, R., Tilly, H., Bouabdallah, R., Morel, P., Van Den Neste, E., Salles, G., Gaulard, P., et al. (2002). CHOP chemotherapy plus rituximab compared with CHOP alone in elderly patients with diffuse large-B-cell lymphoma. *N Engl J Med* 346, 235-242.

- 1 Colell, A., Green, D.R., and Ricci, J.E. (2009). Novel roles for GAPDH in cell death and
2 carcinogenesis. *Cell Death Differ* 16, 1573-1581.
- 3 Copie-Bergman, C., Gaulard, P., Leroy, K., Briere, J., Baia, M., Jais, J.P., Salles, G.A., Berger, F.,
4 Haioun, C., Tilly, H., et al. (2009). Immuno-fluorescence in situ hybridization index predicts survival
5 in patients with diffuse large B-cell lymphoma treated with R-CHOP: a GELA study. *J Clin Oncol* 27,
6 5573-5579.
- 7 Csibi, A., Lee, G., Yoon, S.O., Tong, H., Ilter, D., Elia, I., Fendt, S.M., Roberts, T.M., and Blenis, J.
8 (2014). The mTORC1/S6K1 pathway regulates glutamine metabolism through the eIF4B-dependent
9 control of c-Myc translation. *Current biology : CB* 24, 2274-2280.
- 10 Cunningham, J.T., Rodgers, J.T., Arlow, D.H., Vazquez, F., Mootha, V.K., and Puigserver, P. (2007).
11 mTOR controls mitochondrial oxidative function through a YY1-PGC-1alpha transcriptional complex.
12 *Nature* 450, 736-740.
- 13 Dancey, J. (2010). mTOR signaling and drug development in cancer. *Nat Rev Clin Oncol* 7, 209-219.
- 14 Delarue, R., Tilly, H., Mounier, N., Petrella, T., Salles, G., Thieblemont, C., Bologna, S., Ghesquieres,
15 H., Hacini, M., Fruchart, C., et al. (2013). Dose-dense rituximab-CHOP compared with standard
16 rituximab-CHOP in elderly patients with diffuse large B-cell lymphoma (the LNH03-6B study): a
17 randomised phase 3 trial. *The Lancet. Oncology* 14, 525-533.
- 18 Doherty, J.R., and Cleveland, J.L. (2013). Targeting lactate metabolism for cancer therapeutics. *J Clin*
19 *Invest* 123, 3685-3692.
- 20 Dubois, S., Viailly, P.J., Bohers, E., Bertrand, P., Ruminy, P., Marchand, V., Maingonnat, C.,
21 Mareschal, S., Picquetot, J.M., Penther, D., et al. (2017). Biological and Clinical Relevance of
22 Associated Genomic Alterations in MYD88 L265P and non-L265P-Mutated Diffuse Large B-Cell
23 Lymphoma: Analysis of 361 Cases. *Clin Cancer Res* 23, 2232-2244.
- 24 Duran, R.V., Oppliger, W., Robitaille, A.M., Heiserich, L., Skendaj, R., Gottlieb, E., and Hall, M.N.
25 (2012). Glutaminolysis activates Rag-mTORC1 signaling. *Mol Cell* 47, 349-358.
- 26 Fisher, R.I., Gaynor, E.R., Dahlborg, S., Oken, M.M., Grogan, T.M., Mize, E.M., Glick, J.H.,
27 Coltman, C.A., Jr., and Miller, T.P. (1993). Comparison of a standard regimen (CHOP) with three
28 intensive chemotherapy regimens for advanced non-Hodgkin's lymphoma. *N Engl J Med* 328, 1002-
29 1006.
- 30 Frecha, C., Fusil, F., Cosset, F.L., and Verhoeyen, E. (2011). In vivo gene delivery into hCD34+ cells
31 in a humanized mouse model. *Methods Mol Biol* 737, 367-390.
- 32 Fruman, D.A., and Rommel, C. (2014). PI3K and cancer: lessons, challenges and opportunities. *Nat*
33 *Rev Drug Discov* 13, 140-156.
- 34 Galluzzi, L., Kepp, O., Vander Heiden, M.G., and Kroemer, G. (2013). Metabolic targets for cancer
35 therapy. *Nat Rev Drug Discov* 12, 829-846.
- 36 Gautier, L., Cope, L., Bolstad, B.M., and Irizarry, R.A. (2004). affy--analysis of Affymetrix GeneChip
37 data at the probe level. *Bioinformatics* 20, 307-315.
- 38 Gordan, J.D., Thompson, C.B., and Simon, M.C. (2007). HIF and c-Myc: sibling rivals for control of
39 cancer cell metabolism and proliferation. *Cancer Cell* 12, 108-113.
- 40 Green, T.M., Young, K.H., Visco, C., Xu-Monette, Z.Y., Orazi, A., Go, R.S., Nielsen, O., Gadeberg,
41 O.V., Mourits-Andersen, T., Frederiksen, M., et al. (2012). Immunohistochemical double-hit score is a
42 strong predictor of outcome in patients with diffuse large B-cell lymphoma treated with rituximab plus
43 cyclophosphamide, doxorubicin, vincristine, and prednisone. *J Clin Oncol* 30, 3460-3467.
- 44 Hans, C.P., Weisenburger, D.D., Greiner, T.C., Gascoyne, R.D., Delabie, J., Ott, G., Muller-
45 Hermelink, H.K., Campo, E., Braziel, R.M., Jaffe, E.S., et al. (2004). Confirmation of the molecular

1 classification of diffuse large B-cell lymphoma by immunohistochemistry using a tissue microarray.
2 *Blood* 103, 275-282.

3 Haralambieva, E., Kleiverda, K., Mason, D.Y., Schuurin, E., and Kluin, P.M. (2002). Detection of
4 three common translocation breakpoints in non-Hodgkin's lymphomas by fluorescence in situ
5 hybridization on routine paraffin-embedded tissue sections. *J Pathol* 198, 163-170.

6 Horn, H., Ziepert, M., Becher, C., Barth, T.F., Bernd, H.W., Feller, A.C., Klapper, W., Hummel, M.,
7 Stein, H., Hansmann, M.L., et al. (2013). MYC status in concert with BCL2 and BCL6 expression
8 predicts outcome in diffuse large B-cell lymphoma. *Blood* 121, 2253-2263.

9 Johnson, N.A., Slack, G.W., Savage, K.J., Connors, J.M., Ben-Neriah, S., Rogic, S., Scott, D.W., Tan,
10 K.L., Steidl, C., Sehn, L.H., et al. (2012). Concurrent expression of MYC and BCL2 in diffuse large
11 B-cell lymphoma treated with rituximab plus cyclophosphamide, doxorubicin, vincristine, and
12 prednisone. *J Clin Oncol* 30, 3452-3459.

13 Kheirallah, S., Caron, P., Gross, E., Quillet-Mary, A., Bertrand-Michel, J., Fournie, J.J., Laurent, G.,
14 and Bezombes, C. (2010). Rituximab inhibits B-cell receptor signaling. *Blood* 115, 985-994.

15 Kordes, S., Pollak, M.N., Zwinderman, A.H., Mathot, R.A., Weterman, M.J., Beeker, A., Punt, C.J.,
16 Richel, D.J., and Wilmink, J.W. (2015). Metformin in patients with advanced pancreatic cancer: a
17 double-blind, randomised, placebo-controlled phase 2 trial. *The Lancet. Oncology* 16, 839-847.

18 Lee, M.N., Ha, S.H., Kim, J., Koh, A., Lee, C.S., Kim, J.H., Jeon, H., Kim, D.H., Suh, P.G., and Ryu,
19 S.H. (2009). Glycolytic flux signals to mTOR through glyceraldehyde-3-phosphate dehydrogenase-
20 mediated regulation of Rheb. *Mol Cell Biol* 29, 3991-4001.

21 Lenz, G., and Staudt, L.M. (2010). Aggressive lymphomas. *N Engl J Med* 362, 1417-1429.

22 Lenz, G., Wright, G., Dave, S.S., Xiao, W., Powell, J., Zhao, H., Xu, W., Tan, B., Goldschmidt, N.,
23 Iqbal, J., et al. (2008). Stromal gene signatures in large-B-cell lymphomas. *N Engl J Med* 359, 2313-
24 2323.

25 Lipton, A., Kostler, W.J., Leitzel, K., Ali, S.M., Sperinde, J., Weidler, J., Paquet, A., Sherwood, T.,
26 Huang, W., Bates, M., et al. (2010). Quantitative HER2 protein levels predict outcome in fluorescence
27 in situ hybridization-positive patients with metastatic breast cancer treated with trastuzumab. *Cancer*
28 116, 5168-5178.

29 Mackay, G.M., Zheng, L., van den Broek, N.J., and Gottlieb, E. (2015). Analysis of Cell Metabolism
30 Using LC-MS and Isotope Tracers. *Methods Enzymol* 561, 171-196.

31 Mareschal, S., Ruminy, P., Bagacean, C., Marchand, V., Cornic, M., Jais, J.P., Figeac, M., Picquetot,
32 J.M., Molina, T.J., Fest, T., et al. (2015). Accurate Classification of Germinal Center B-Cell-
33 Like/Activated B-Cell-Like Diffuse Large B-Cell Lymphoma Using a Simple and Rapid Reverse
34 Transcriptase-Multiplex Ligation-Dependent Probe Amplification Assay: A CALYM Study. *J Mol*
35 *Diagn.*

36 Meynet, O., and Ricci, J.E. (2014). Caloric restriction and cancer: molecular mechanisms and clinical
37 implications. *Trends in molecular medicine.*

38 Molina, T.J., Canioni, D., Copie-Bergman, C., Recher, C., Briere, J., Haioun, C., Berger, F., Ferme,
39 C., Copin, M.C., Casasnovas, O., et al. (2014). Young patients with non-germinal center B-cell-like
40 diffuse large B-cell lymphoma benefit from intensified chemotherapy with ACVBP plus rituximab
41 compared with CHOP plus rituximab: analysis of data from the Groupe d'Etudes des Lymphomes de
42 l'Adulte/lymphoma study association phase III trial LNH 03-2B. *J Clin Oncol* 32, 3996-4003.

43 Monti, S., Savage, K.J., Kutok, J.L., Feuerhake, F., Kurtin, P., Mihm, M., Wu, B., Pasqualucci, L.,
44 Neuberg, D., Aguiar, R.C., et al. (2005). Molecular profiling of diffuse large B-cell lymphoma
45 identifies robust subtypes including one characterized by host inflammatory response. *Blood* 105,
46 1851-1861.

1 Morita, M., Gravel, S.P., Chenard, V., Sikstrom, K., Zheng, L., Alain, T., Gandin, V., Avizonis, D.,
2 Arguello, M., Zakaria, C., et al. (2013). mTORC1 controls mitochondrial activity and biogenesis
3 through 4E-BP-dependent translational regulation. *Cell metabolism* 18, 698-711.

4 Nicholson, J.K., Foxall, P.J., Spraul, M., Farrant, R.D., and Lindon, J.C. (1995). 750 MHz ¹H and ¹H-
5 ¹³C NMR spectroscopy of human blood plasma. *Analytical chemistry* 67, 793-811.

6 Norberg, E., Lako, A., Chen, P.H., Stanley, I.A., Zhou, F., Ficarro, S.B., Chapuy, B., Chen, L., Rodig,
7 S., Shin, D., et al. (2017). Differential contribution of the mitochondrial translation pathway to the
8 survival of diffuse large B-cell lymphoma subsets. *Cell Death Differ* 24, 251-262.

9 Petrella, T., Copie-Bergman, C., Briere, J., Delarue, R., Jardin, F., Ruminy, P., Thieblemont, C.,
10 Figeac, M., Canioni, D., Feugier, P., et al. (2017). BCL2 expression but not MYC and BCL2
11 coexpression predicts survival in elderly patients with diffuse large B-cell lymphoma independently of
12 cell of origin in the phase 3 LNH03-6B trial. *Ann Oncol* 28, 1042-1049.

13 Poste, G. (2011). Bring on the biomarkers. *Nature* 469, 156-157.

14 Ricci, J.E., and Chiche, J. (2018). Metabolic Reprogramming of Non-Hodgkin's B-Cell Lymphomas
15 and Potential Therapeutic Strategies. *Front Oncol* 8, 556.

16 Rustin, P., Chretien, D., Bourgeron, T., Gerard, B., Rotig, A., Saudubray, J.M., and Munnich, A.
17 (1994). Biochemical and molecular investigations in respiratory chain deficiencies. *Clin Chim Acta*
18 228, 35-51.

19 Sehn, L.H., and Gascoyne, R.D. (2015). Diffuse large B-cell lymphoma: optimizing outcome in the
20 context of clinical and biologic heterogeneity. *Blood* 125, 22-32.

21 Swerdlow, S.H., Campo, E., Pileri, S.A., Harris, N.L., Stein, H., Siebert, R., Advani, R., Ghielmini,
22 M., Salles, G.A., Zelenetz, A.D., et al. (2016). The 2016 revision of the World Health Organization
23 classification of lymphoid neoplasms. *Blood* 127, 2375-2390.

24 Wheaton, W.W., Weinberg, S.E., Hamanaka, R.B., Soberanes, S., Sullivan, L.B., Anso, E., Glasauer,
25 A., Dufour, E., Mutlu, G.M., Budigner, G.S., et al. (2014). Metformin inhibits mitochondrial complex
26 I of cancer cells to reduce tumorigenesis. *Elife* 3, e02242.

27 Willems, L., Jacque, N., Jacquel, A., Neveux, N., Maciel, T.T., Lambert, M., Schmitt, A., Poulain, L.,
28 Green, A.S., Uzunov, M., et al. (2013). Inhibiting glutamine uptake represents an attractive new
29 strategy for treating acute myeloid leukemia. *Blood* 122, 3521-3532.

30 Wishart, D.S., Jewison, T., Guo, A.C., Wilson, M., Knox, C., Liu, Y., Djoumbou, Y., Mandal, R.,
31 Aziat, F., Dong, E., et al. (2013). HMDB 3.0--The Human Metabolome Database in 2013. *Nucleic*
32 *Acids Res* 41, D801-807.

33

34

1 **Figure titles and legends**

2

3 **Figure 1. DLBCLs expressing low levels of GAPDH are associated with a poor response to R-**
4 **CHOP treatment and with OxPhos metabolism.**

5 **A.** Distribution of *gapdh* expression values (log₂ mRNA intensity) in newly diagnosed DLBCLs
6 characterized as DLBCLs-*gapdh*^{low} (n=125) and DLBCLs-*gapdh*^{high} (n=108) (analysis from (Lenz et
7 al., 2008). p value from Wilcoxon rank sum.

8 **B.** Overall survival (OS) of R-CHOP-treated DLBCL patients, according to *gapdh*^{low} (n=125) and
9 *gapdh*^{high} (n=108) mRNA levels in DLBCL biopsies at diagnosis (analysis from (Lenz et al., 2008). p
10 value from log-rank test.

11 **C.** Illustration of IHC staining of GAPDH in germinal center (GC) B cells of a reactive lymph node
12 (LN) (score = 80) and in *de novo* DLBCL expressing low (score = 80) or high (score = 260) levels of
13 GAPDH protein. Magnification 20X (100 μm).

14 **D.** Distribution of GAPDH protein expression scored by IHC in GCB cells from human paraffin-
15 embedded reactive lymph nodes (n=5) or newly diagnosed DLBCLs expressing low (score ≤ 150;
16 n=15) or high (score > 150; n=28) GAPDH protein (Training cohort). p value from Wilcoxon rank
17 sum.

18 **E.** OS of R-CHOP-treated DLBCL patients according to the levels of GAPDH expression determined
19 by IHC in newly diagnosed DLBCLs (n=15 GAPDH^{low} and n=28 GAPDH^{high}; Training cohort). p
20 value from log-rank test.

21 **F.** Distribution of GAPDH protein expression scored by IHC staining of GAPDH in tissue-microarray
22 corresponding to 294 paraffin-embedded *de novo* DLBCL biopsies. 204 DLBCLs-GAPDH^{low} and 90
23 DLBCLs-GAPDH^{high} are identified (validation cohort). p value from Wilcoxon rank sum.

24 **G.** OS of 294 R-CHOP-treated patients with DLBCLs grouped on the basis of GAPDH expression
25 levels presented in **F**. p value from log-rank test.

26 **H.** Transcript abundance (probe intensity) of *gapdh* mRNA according to the CCC classification (n=82
27 BCR-DLBCL and n=71 OxPhos-DLBCL) identified by genomic clustering (Monti et al., 2005),
28 analysis from ((Lenz et al., 2008). p value from Wilcoxon test.

1 **I.** Correlation between GAPDH expression levels scored by IHC and glycolytic ATP in malignant B
2 cells harvested from patients with newly diagnosed DLBCLs. Blue dots represent DLBCLs-
3 GAPDH^{low} (n=3) and red dots represent DLBCL-GAPDH^{high} (n=8). R, Pearson correlation coefficient.
4 p value from correlation test.

5 See also Tables S1, S2, S3 and Figures S1 and S2, related to Figure 1.

6

7 **Figure 2. Mouse primary B lymphomas expressing low levels of GAPDH rely on OxPhos**
8 **metabolism and are sensitive to inhibition of the electron transport chain complex I activity.**

9 **A.** Quantification of intracellular ATP levels produced in E μ -Myc-GAPDH^{low} and in E μ -Myc-
10 GAPDH^{high} cells (n=5 independent lymphomas per group). Results are expressed as relative
11 luminescence units normalized by live cell number.

12 **B.** Glycolytic ATP production measured as the percentage of total ATP produced by E μ -Myc-
13 GAPDH^{low} and E μ -Myc-GAPDH^{high} cells (n=5 independent lymphomas per group). Data are
14 expressed as mean \pm s.d (n=3 independent experiments).

15 **C.** Lactate secretion was determined in the supernatant of E μ -Myc-GAPDH^{low} and of E μ -Myc-
16 GAPDH^{high} cells (n=5 independent lymphomas per group), 24 hours after seeding (mean \pm s.d; n=3
17 independent experiments).

18 **D.** Baseline oxygen consumption rate (OCR) of E μ -Myc-GAPDH^{low} and of E μ -Myc-GAPDH^{high} cells
19 was determined with Clarck electrode 24 hours after seeding (n=5 independent lymphomas/group).
20 Data are expressed as mean \pm s.d (n=3 independent experiments).

21 **E.** E μ -Myc-GAPDH^{low} and E μ -Myc-GAPDH^{high} cells (n=3 independent lymphomas/group) were
22 seeded in the presence or absence (Ctl, DMSO) of phenformin (Phen, 300 μ M) for 24 hours. Cell
23 death was determined by DAPI staining and analyzed by flow cytometry. Data are expressed as mean
24 \pm s.d (n=4 independent experiments).

25 **F. G.** Kaplan–Meier curves for the survival of syngeneic C57BL/6 mice intravenously injected with
26 primary E μ -Myc-GAPDH^{low} (**F.**) or E μ -Myc-GAPDH^{high} (**G.**) cells and treated six days later, with
27 either vehicle (H₂O) or 100 mg/kg/day of Phenformin, orally and daily during 3 weeks (n=10
28 mice/group, p value from log-rank test, *** p< 0.001).

1 From panels **A.** to **E.**, *** $p < 0.001$ indicated significance of the observed differences. *ns*, not
2 significant.

3 See also Figures S3 and S4, related to Figure 2.
4

5 **Figure 3. Active mTORC1 signaling in B lymphomas expressing low levels of GAPDH is**
6 **implicated in OxPhos metabolism.**

7 **A.** Whole-cell lysates prepared from E μ -*Myc* cells harvested from independent E μ -*Myc* lymphomas
8 were analyzed by immunoblot with the indicated antibodies. Each lane represents an independent
9 lymphoma. Erk2 is used as a loading control.

10 **B.** Representative immunohistochemistry slides of *de novo* DLBCL biopsies stained for GAPDH and
11 P-p70S6K (T389) proteins. Magnification 20X (100 μ m). Table represents the summary of the
12 GAPDH and P-p70S6K (T389) stained slides for 18 *de novo* DLBCL biopsies. *p* value from Fisher
13 test.

14 **C.** E μ -*Myc*-GAPDH^{low} cells (lymphomas #F) were seeded in the presence or absence (Ctl, DMSO) of
15 10 nM and 20 nM of Rapamycin for 15 hours. Whole-cell lysates were then analyzed for the indicated
16 proteins. Erk2 was used as a loading control.

17 **D-F.** Baseline OCR (**D.**), maximal respiration (**E.**) and ATP-coupled OCR (**F.**) of E μ -*Myc*-GAPDH^{low}
18 cells (lymphoma #F) pre-treated or not (Ctl, DMSO) with indicated doses of Rapamycin for 15 hours
19 were determined with Seahorse XF96 Extracellular Flux Analyzer. Maximal respiration (**E.**) is
20 immediately determined after injection of 0.5 μ M of FCCP. ATP-coupled OCR (**F.**) represents
21 oligomycin-sensitive respiration. Data are expressed as mean \pm s.d. (n=3 independent experiments, in
22 quadruplicates).

23 **G.** Glycolytic ATP production measured as the percentage of total ATP in E μ -*Myc*-GAPDH^{low} cells
24 (lymphoma #F) incubated in the presence or absence (Ctl, DMSO) of 10 nM and 20 nM of Rapamycin
25 for 15 hours, was quantified using a luciferin/luciferase-based assay. The presented data are expressed
26 as mean \pm s.d. (n=2 independent experiments).

27 **H.** E μ -*Myc*-GAPDH^{low} and E μ -*Myc*-GAPDH^{high} cells (n=3 independent lymphomas/group) were
28 seeded in the presence or absence (Ctl, DMSO) of indicated doses of Rapamycin for 15, 24 and 48

1 hours. Cell death was determined by DAPI staining and analyzed by flow cytometry. Data are
2 expressed as mean \pm s.d (n=2 independent experiments).

3 **I.** Survival of syngeneic C57BL/6 mice intravenously injected with primary E μ -Myc-GAPDH^{low} cells
4 (isolated from lymphoma #F) and treated six days later with either vehicle (NaCl 0.9%-5%Tween-5%
5 PEG-200-1% EtOH) or Temsirolimus (10 mg/kg) intraperitoneally two times per week (n=6
6 mice/group, p value from log-rank, ***p< 0.001).

7 **J.** Whole-cell lysates prepared from axillary lymph node tumors of Vehicle or Temsirolimus
8 (10 mg/kg) treated E μ -Myc-GAPDH^{low}-bearing mice were analyzed by immunoblot for the indicated
9 antibodies. Each lane represents an independent mouse. *n.s* means non-specific band. Erk2 is used as a
10 loading control. ***p<0.001 indicated significance of the observed differences.

11 See also Figures S5, related to Figure 3.

12

13 **Figure 4. Mouse primary B lymphomas expressing low levels of GAPDH rely on glutamine**
14 **metabolism and are sensitive to hydrolysis of extracellular glutamine by *E-Coli* L-asparaginase.**

15 **A.** Glutamine consumption was determined in the supernatant of E μ -Myc-GAPDH^{low} and E μ -Myc-
16 GAPDH^{high} cells (n=5 independent lymphomas per group), 24 hours after seeding.

17 **B.** Glutamine transport rates (in cpm) is measured in 5.10⁶ E μ -Myc-GAPDH^{low} or E μ -Myc-GAPDH^{high}
18 cells (n=4 independent lymphomas/group) incubated for 30 minutes in an amino-acid-free, 20 mM
19 glucose containing DMEM supplemented with [¹⁴C]-Glutamine. Data are expressed as mean \pm s.d
20 (n=2 independent experiments in triplicate).

21 **C.** Heat map depicting significantly changed glycolytic/ non-oxidative pentose phosphate pathway
22 (PPP) and glutaminolysis/ tricarboxylic acid (TCA) cycle metabolite levels in E μ -Myc-GAPDH^{low} and
23 in E μ -Myc-GAPDH^{high} cells (n=3 independent lymphomas per group, four replicates per lymphoma)
24 24 hours after seeding, as analyzed by LC-MS. Red, increase; blue, decrease.

25 **D.** Whole-cell lysates prepared from E μ -Myc-GAPDH high and low cells were analyzed by
26 immunoblot for the mitochondrial glutaminase (GLS). Erk2 is used as a loading control.

27 **E.** Concentration of glutamine (left panel) and of asparagine (right panel) in the supernatant of E μ -
28 Myc-GAPDH high (in red) and low (in bleu) cells (n=4 independent lymphomas per group) treated or

1 not (Ctl) with *E-Coli* L-asparaginase (L-ase) at indicated doses for 4 hours. The presented data are
2 expressed as mean \pm s.d (n=3 independent experiments).

3 **F.** E μ -Myc-GAPDH^{low} and E μ -Myc-GAPDH^{high} cells (n=3 independent lymphomas/group) were
4 seeded in the presence or absence (Ctl) of *E-Coli* L-asparaginase (L-ase, at indicated doses) for 15
5 hours. Cell death was determined by DAPI staining and analyzed by flow cytometry (n=3 independent
6 experiments).

7 **G.** Plasma glutamine concentration 4 hours after the last *ip* administration of NaCl 0.9% (Ctl) or *E-*
8 *Coli* L-asparaginase (L-ase, 2500 IU/kg) in E μ -Myc-GAPDH^{low}- and in E μ -Myc-GAPDH^{high}-bearing
9 mice (n=4 mice per group).

10 **H. I.** Survival of syngeneic C57BL/6 mice intravenously injected with primary E μ -Myc-GAPDH^{low}
11 (**H.**) or E μ -Myc-GAPDH^{high} cells (**I.**) and treated six days later with either vehicle (NaCl 0.9%) or
12 2500 IU/kg of *E-Coli* L-asparaginase (L-ase) intraperitoneally five times per week the first week and
13 three times per week the following weeks (n=6 mice/group, p value from log-rank, ***p< 0.001).

14 From panel **A.** to **G.**, **p< 0.01, ***p<0.001 indicated significance of the observed differences. *ns*,
15 not significant.

16 See also Figure S6, related to Figure 4.

17

18 **Figure 5. Specific overexpression of human GAPDH reduces mTORC1 signaling and decreases**
19 **B lymphomas sensitivity to phenformin or *E-Coli* L-asparaginase *in vivo*.**

20 **A.** Total cell extracts from mouse primary E μ -Myc-GAPDH^{low} cells (lymphoma #F) stably transduced
21 with control (pMIG) or GAPDH-V5-encoding pMIG vectors were immunoblotted for the indicated
22 proteins. Erk2 is used as a loading control.

23 **B.** Intracellular ATP levels produced in E μ -Myc-GAPDH^{low} cells stably overexpressing GAPDH-V5
24 or control vector (pMIG) were quantified using a luciferin/luciferase-based assay and results were
25 expressed as relative luminescence units normalized by cell number (n=3 independent experiments).

26 **C.** Glycolytic ATP production was measured as the percentage of total ATP in cells presented in **A.**
27 Data are presented as means \pm s.d (n=3 independent experiments).

1 **D.** Lactate production was determined in the supernatant of mouse primary E μ -Myc-GAPDH^{low} cells
2 (lymphoma #F) stably transduced with control (pMIG) or GAPDH-V5-encoding pMIG vectors, 24
3 hours after seeding. Data are presented as mean \pm s.d (n=3 independent experiments).

4 **E.** Baseline OCR of cells presented in **A.** was determined with Clarck electrode, 24 hours after cell
5 seeding. Data are expressed as mean \pm s.d (n=3 independent experiments).

6 **F.** Glutamine consumption was determined 24 hours after cell seeding in the supernatant of E μ -Myc-
7 GAPDH^{low} cells (lymphoma #F) stably transduced with control (pMIG) or GAPDH-V5-encoding
8 pMIG vectors. Data are expressed as mean \pm s.d (n=3 independent experiments).

9 **G.** Weight of inguinal (left) and axillary (right) lymphomas harvested from wild-type syngeneic
10 C57BL/6 mice twenty days after intravenous injection of primary E μ -Myc-GAPDH^{low} cells stably
11 over-expressing or not (pMIG) GAPDH-V5. Phenformin (100 mg/kg/day) or vehicle (H₂O) were
12 administrated every day for the last thirteen days (pMIG-Vehicle, n=8; pMIG-Phenformin, n=9;
13 GAPDH-V5-Vehicle, n=10; GAPDH-V5-Phenformin, n=7).

14 **H. I.** Survival of syngeneic C57BL/6 mice intravenously injected with primary E μ -Myc-GAPDH^{low}
15 cells stably transduced with control pMIG vector (**H.**) or GAPDH-V5-encoding pMIG vectors (**I.**) and
16 treated six days later with either vehicle (NaCl 0.9%) or 2500 IU/kg of E-Coli L-asparaginase (L-ase)
17 intraperitoneally five times per week the first week and three times per week the following weeks
18 (n=10 mice/group, p value from log-rank, **p< 0.01; ***p< 0.001).

19 From panel **A.** to **G.**, *p<0.05, **p<0.01, ***p<0.001 indicated significance of the observed
20 differences. *ns*, not significant.

21 See also Figure S7, related for Figure 5.

22

23 **Figure 6. Patients with DLBCL-GAPDH^{low} are sensitive to specific inhibitors of mitochondrial**
24 **metabolism (KTM treatment).**

25 **A.** Schematic representation of conventional therapeutic protocol for patients with DLBCL. Once
26 diagnosed, patients with DLBCL receive immuno-chemotherapy, R-CHOP. Approximately, 40% of
27 the patients will experience therapeutic failure (refractory or relapse). Other anti-CD20-based
28 therapies such as R-DHAP (Rituximab, dexamethasone-Ara-C (cytarabine)-Platinol (cisplatin)) or R-

1 ICE (Rituximab, Ifosfamide-Carboplatin-Etoposide) are then proposed. Another set of 40% of patients
2 will not respond to those treatments and will be eligible for HDT/ASCT (High Dose Therapy with
3 Autologous Stem Cell Transplantation). In the case of *de novo* DLBCL-GAPDH^{low} (low responders to
4 R-CHOP), we propose a clinical protocol called KTM (Kidrolase-Torisel-Metformin), to interfere
5 with tumor metabolism upon relapse of all anti-CD20-based therapies.

6 **B.** Schematic representation of one cycle of KTM therapy. 4 weeks-cycle of KTM consisted in the
7 combination of *E-Coli* L-asparaginase (K, Kidrolase® 6000 UI/m²) on days 1, 3, 5, 7, 9, 11, and 13,
8 mTOR inhibitor temsirolimus (T, Torisel 75 mg D1, 7, 14) and Metformin (1000 mg/day) on day 14
9 to day 28. Four patients with DLBCL-GAPDH^{low} at diagnosis and refractory to all anti-CD20-based
10 therapies, were eligible to KTM therapy.

11 **C.** Progressive regression of the patient #1's DLBCL (CD10⁺, bcl2⁺, Mum1⁻, Ki67⁺ 80%, MYC⁺, Ann
12 Arbor Stage IV) upon KTM treatment.

13 **D.** 3D modelization of Computed Tomography (CT) scan of patient #1 before (T=0) and after (T=30
14 days) two cycles of KTM treatment.

15 **E.** Illustration of GAPDH expression (and respective GAPDH IHC score) in DLBCL biopsies at
16 diagnosis, from the four patients enrolled in the KTM study.

17 **F.** Duration of treatment and therapeutic response (by CT or PET) to KTM for the four individual
18 patients presenting DLBCL-GAPDH^{low} at diagnosis (**E.**).

19 KTM, Kidrolase, Torisel and Metformin; CR, complete response; PR, partial response; PD,
20 progressive disease; PAC, patient alive at last consultation; AE, adverse event.

21 See also Table S4 related to Figure 6.

22

23 **Tables with titles and legends,**

24 **Table 1. GAPDH expression levels are not associated with other biological prognostic factors.**

25 BCL2 ≥ 70% means that 70% (or more) of malignant B cells stained for BCL2 protein by IHC (Green
26 et al., 2012; Petrella et al., 2017); BCL6 > 25% means up to 25% of malignant B cells stained for
27 BCL6 by IHC (Horn et al., 2013); MYC ≥ 40% (Johnson et al., 2012) means that 40% (or more) of

1 malignant B cells stained for MYC protein by IHC. Double hit (*MYC/BCL2*) and triple hit
2 (*MYC/BCL2/BCL6*) were obtained by Fluorescence In Situ Hybridization (FISH).
3 *p* value from Fisher test. See also Tables S2 and S3, related to Table 1.

4 **STAR Methods**

6 **CONTACT FOR REAGENT AND RESOURCE SHARING**

7 Further information and requests for resources and reagents should be directed to and will be fulfilled
8 by the Lead Contact, Jean-Ehrland Ricci (ricci@unice.fr).

9 10 11 **Materials and Methods**

13 **Experimental model and subject details**

14 *Mice and in vivo studies using Eμ-Myc cells*

15 C57BL/6 Eμ-Myc transgenic mice were purchased from the Jackson Laboratory (#002728) and
16 housed in our local animal facility (C3M, Nice, France).

17
18 The lymphoma transfer of Eμ-Myc cells was performed into syngeneic, nontransgenic, 6-weeks-old
19 C57BL/6J0laHsd females (Envigo) by intravenous injection (*iv*) of 0.1×10^6 viable Eμ-Myc
20 lymphoma cells per recipient mouse (in 150 μl of sterile PBS). Six days after cell injection, mice
21 received treatments. 100 mg/kg/day of Phenformin (P7045, Sigma-Aldrich) or vehicle (H₂O) (n=10
22 mice/group) were administrated by gavage (*p.o*) every day for three weeks. 2500 UI/kg/day of *E-Coli*
23 L-asparaginase (Kidrolase, L-ase, Jazz Pharmaceutical) or vehicle (NaCl 0.9%) was injected
24 intraperitoneally for five days the first week and three times per week the following weeks, for a total
25 of three weeks of treatment (n=6 mice/group). 10 mg/kg of Temsirolimus (PZ0020, Sigma-Aldrich) or
26 vehicle (NaCl 0.9%-5% Tween-5% PEG-200-1% EtOH) were intraperitoneally injected two times per
27 week for three weeks (n=6 mice per group). Tumor onset was determined by inguinal lymph node
28 palpation. Lymphoma-bearing animals were sacrificed by cervical dislocation. Phenformin-treated

1 mice were sacrificed two hours after the last gavage of phenformin to analyze effects of the compound
2 on lymphoma cell signaling. *E-Coli* L-asparaginase (L-ase) treated mice were sacrificed four hours
3 after the last *ip* injection of L-ase and plasma was immediately isolated to analyze plasma glutamine
4 concentrations. Temsirolimus treated mice were sacrificed 24 hours after the last treatment to analyze
5 *in vivo* efficacy of this compound within the lymphomas.

6 All mice were maintained in specific pathogen-free conditions and all experimental procedures were
7 approved by the national Animal Care and Use Committee and the regional ethics committee
8 (05111.02 from Direction Générale de la Recherche et de l'Innovation). Survival was determined as
9 the time between the *i.v.* injection of the cells and the time when mice had to be sacrificed, as soon as
10 they exhibit systemic signs of illness (apathy, hair loss, breathing problems, precipitous weight loss,
11 and limited ability to reach food or water), in agreement with the guidelines of the Institutional Animal
12 Care and Use Committee. Food was given *ad libitum*. Experiments using the E μ -Myc cells
13 transplantation in syngeneic C57BL/6 mice have shown statistical significance starting from 6
14 mice/group. No randomization was performed. Endpoint was evaluated by blinding.

15

16 ***Cell lines and culture conditions***

17 Mouse primary E μ -Myc lymphomas cells were isolated from different C57BL/6 E μ -Myc transgenic
18 mice as previously described (Chiche et al., 2015) and maintained in DMEM-GlutamaX (#31966047,
19 Thermo Fisher Scientific) supplemented with 10% FBS, 50 μ M of 2-mercaptoethanol (#31350010,
20 Thermo Fisher Scientific), 0.37 mM of L-asparagine (A0884, Sigma-Aldrich) and 10 mM of HEPES
21 pH 7.4 (#15630056, Thermo Fisher Scientific).

22

23 The human DLBCL cell lines Toledo, Karpas 422, SU-DHL-4 and SU-DHL-6 were tested
24 mycoplasma-free. Cell line authentication was performed by DSMZ by DNA profiling using 8
25 different and highly polymorphic short tandem repeat (STR) loci. There was also no presence of
26 mitochondrial DNA sequences from rodent cells as mouse, rat, Chinese and Syrian hamster. The

1 Karpas 422 cell line was from the ECACC (European Collection of Authenticated Cell cultures), the
2 Toledo cell line was from ATCC (American Type Culture Collection), the SU-DHL-4 and SUD-HL-6
3 cell lines were from DSMZ (German Collection of Microorganisms and Cell Culture). Toledo, Karpas
4 422 and SU-DHL-4 cells were maintained in RPMI-GlutamaX (#61870044, Thermo Fisher
5 Scientific), supplemented with 10% FBS. SU-DHL-6 cells were maintained in RPMI-GlutamaX
6 supplemented with 20% FBS.

7

8 ***Microarray data analysis***

9 Raw.CEL files and clinical information from the study of Lenz G. *et al.* (Lenz et al., 2008). were
10 downloaded from the Gene Expression Omnibus database (GSE10846). The total number of samples
11 included in this study was 414, 181 treated with CHOP and 233 with R-CHOP. Data were
12 summarized, normalized and log2 transformed using the justRMA function from the Bioconductor
13 package affy (version 1.40.0, (Gautier et al., 2004)). Follow-up time was limited to 5 years.
14 Association between gene expression levels and overall survival was performed on samples from the
15 R-CHOP arm only. Samples with low expression levels were filtered out (\log_2 intensity < 8). For each
16 remaining probeset, samples were split into two groups (below and above the median) and difference
17 in survival was assessed using Cox proportional hazards models. 587 candidate probesets were
18 selected based on nominal p-value < 0.05 and an $\text{abs}(\log_2 \text{HR}) > 0.75$.

19 Association of expression levels with OS was first tested by categorizing samples into high/low
20 expression samples using median values. Then for *gapdh*, cutoff was optimized using positional
21 scanning (Lipton et al., 2010). Survival curves were plotted following the Kaplan and Meier method,
22 and statistical significance was assessed using the log-rank test. Survival analysis was performed using
23 functions from the R package survival.

24 OxPhos and BCR classification were obtained from the supplemental data of (Caro et al., 2012).
25 Statistical significance was assessed using Wilcoxon rank sum test. Enrichment in biological themes
26 (Molecular function and canonical pathways) were performed using Ingenuity Pathway Analysis

1 software.

2

3 ***DLBCL patients: Training & Validation cohorts***

4 DLBCL tumors were required to be *de novo* and treated with Rituximab-CHOP (R-CHOP). All cases
5 were diagnosed and reviewed by experienced hematopathologists and patient clinical information
6 were obtained from the Hospital Saint Louis, Centre Hospitalier Princesse Grace and Centre Antoine
7 Lacassagne institutions. DLBCLs were classified according to the WHO classification. Clinical data
8 including gender, age, and age-adjusted International Prognosis Index (IPIaa) (scored (0-1, 2 and 3)
9 based on i) the Ann Arbor stage (II-II vs III-IV), ii) the level of lactate dehydrogenase in the serum
10 (LDH \leq normal vs \geq normal) and iii) the Performance status (PS 0-1 vs 2-4)) were collected in all
11 cases and are summarized in Table S2. These cases were anonymized and processed in accordance
12 with a protocol approved by scientific committee of the LYSA (The Lymphoma Study Association).
13 All patients gave written non-opposition consent. Patients samples were allocated to GAPDH high and
14 low groups according to their respective expression (see GAPDH IHC staining and scoring section).

15 *Training cohort.* A total of 43 patients aged >18 years (aged between 24-85 years) who had been
16 diagnosed with *de novo* DLBCL and then treated with Rituximab and CHOP between 2008 and 2014
17 at Onco-Hematology Department of Nice CHU (France) and Saint-Louis Hospital, APHP, Paris
18 (France) were included in this training set. The samples were prepared from the paraffin blocks of
19 lymph nodes that were recovered from the archives of the Pathology departments.

20 *Validation cohort.* All cases analyzed in the validation cohort were enrolled in the prospectively
21 randomized phase 3 multi-center GELA-LNH03-6B trial (Delarue et al., 2013) in which 602 patients
22 with untreated diffuse large B-cell lymphomas (DLBCLs) and at least one adverse prognostic factor
23 aged between 60-80 years had been randomly assigned to receive eight cycles of R-CHOP-14 or eight
24 cycles of R-CHOP-21. They did not show any difference in efficacy endpoints between dose-dense
25 and standard regimens of R-CHOP. 294 biopsies specimens at diagnosis were available for the tissue
26 microarray (TMA). TMA contains three representative 0.6-mm cores of routinely processed tissues

1 (Beecher Instruments, Silver Spring, MD).

2

3 ***Clinical protocol KTM (Kidrolase-Torisel-Metformin)***

4 Four patients harboring *de novo* Myc-translocated-DLBCLs and selected for KTM treatment presented
5 i) a retrospective GAPDH^{low} levels (scored by IHC in diagnosed biopsies), ii) a therapeutic failure
6 after a median of 2 prior lines of Rituximab-based therapies and iii) adequate performance status and
7 organ functions. KTM treatment consisted in L-asparaginase (K, Kidrolase®, Jazz Pharamaceutical,
8 6000 UI/m²) on days 1, 3, 5, 7, 9, 11, and 13, mTOR inhibitor (T, Torisel, Pfizer, 75 mg) on days 1, 7
9 and 14, and Metformin (Mylan, 1000 mg/day) on day 14 to day 28. **The study was approved on Oct**
10 **16th, 2012 by the Scientific Committee of the LYSA (The Lymphoma Study Association, reference:**
11 **REMtor).** All patients gave a written informed consent to receive the treatment. Consent to publish
12 patients' images was obtained. There was no clinical trial registration number because the therapeutic
13 protocol was conducted on a local cohort.

14

15 **Methods details**

16

17 ***COO classification***

18 Frozen tissues were analyzed using GeneChip Human Genome HGU133 Plus 2.0 arrays (Affymetrix,
19 Santa Clara) as previously reported (Dubois et al., 2017). From the LNH03-6B TMA (validation
20 cohort), sixty DLBCLs had both COO molecular classification.

21 Reverse transcription-multiplex ligation-dependent probe amplification (RT-MLPA) was performed to
22 determine the COO on thirty-five formalin-fixed paraffin-embedded (FFPE) DLBCLs (training
23 cohort), using a targeted molecular gene expression approach as recently described (Mareschal et al.,
24 2015).

25

1 ***GAPDH immunohistochemical (IHC) staining and scoring.***

2 Sections (4 μm) of formalin-fixed, paraffin-embedded DLBCL biopsies (training cohort) or tissue-
3 microarray (TMA) from the LYSA group (validation cohort) were treated for deparaffinization,
4 rehydration, and antigen retrieval using standard procedures (EnVision™ FLEX reagents, Agilent,
5 Dako). Before immunohistochemistry, antigen retrieval was performed at pH 9.0, for 20 minutes at
6 97°C, according to the manufacturer's instructions (EnVision™ FLEX reagents, Agilent, Dako). After
7 washing in diluted EnVision FLEX Wash Buffer, slides were incubated in EnVision FLEX
8 Peroxidase-Blocking Reagent solution for 5 min to quench endogenous peroxidase. Slides were then
9 washed, stained at room temperature on an automated system (Autostainer link 48, Dako) with diluted
10 (EnVision FLEX antibody diluent) anti-GAPDH (rabbit polyclonal anti-human GAPDH, HPA40067,
11 Sigma-Aldrich; dilution 1:500) for 20 minutes, washed, incubated 20 minutes with Dako EnVision™
12 FLEX /HRP), washed, incubated 8 minutes with EnVision FLEX Substrate Working solution and
13 counter-stained with Hematowlylin (EnVision™ FLEX Hematoxylin). Sections were then dehydrated
14 and mounted with pertex (Histolab).

15 Cytoplasmic GAPDH IHC staining was blindly scored by two pathologists from the LCAP from Nice
16 CHU (Dr D. Ambrosetti and Dr. J. Reverso-Meinietti) based on two parameters: the GAPDH IHC
17 staining intensity in tumor cells (scored 0 for absence of staining, 1 for a weak staining, 2 for a
18 medium staining and 3 for a strong staining) and the proportion of tumor cells displaying each
19 intensity. Then GAPDH IHC score was obtained by multiplying each GAPDH staining intensity with
20 the corresponding percentage of tumor cells stained (example: GAPDH IHC score= 0 (non-stained) x
21 % tumor cells + 1 (weak intensity) x % tumor cells stained + 2 (medium intensity) x % tumor cells
22 stained + 3 (strong intensity) x % tumor cells stained). For the training cohort, GAPDH IHC staining
23 was scored on the whole slide. For the TMA, GAPDH IHC score represents the mean of three
24 different tissue spots from the same tumor. GAPDH IHC cut off of 150 was determined using
25 positional scanning (Lipton et al., 2010). Illustrations of GAPDH IHC staining were performed using
26 SlidePath Digital Image software (Leica Biosystems).

27

1 *Immunohistochemistry and fluorescence in situ hybridization*

2 Sections (4 µm) of formalin-fixed, paraffin-embedded DLBCL biopsies (training cohort) were treated
3 for deparaffinization, rehydration, and antigen retrieval using standard procedures (EnVision™ FLEX
4 reagents, Agilent, Dako). Antibodies against CD5 (M3641, Agilent, Dako), CD79A (M7050, Agilent,
5 Dako), CD20 (M0755, Agilent, Dako), CD10 (GA64861-2, Agilent, Dako), BCL2 (M0887, Agilent,
6 Dako), BCL6 (M7211, Agilent, Dako), MUM1 (M7259, Agilent, Dako), c-MYC (ab32072, Abcam)
7 and phospho-p70S6K (T389) (rabbit monoclonal anti-phospho-p70S6K (T389), #9234, Cell Signaling
8 Technology) were used for immunostainings performed on an automated system (Autostainer link 48,
9 Dako). Antigen retrieval was performed at specific pH prior incubation with indicated antibodies: pH
10 6.0 prior anti-CD79A, anti-CD20, anti-MUM1 and pH 9.0 prior anti-CD5, anti-CD10, anti-BCL2,
11 anti-BCL6, anti-c-Myc and anti-phospho-p70S6K (T389). Primary antibodies were diluted in
12 EnVision FLEX antibody diluent (anti-CD5, anti-CD10, anti-CD20, anti-BCL2 are prediluted; anti-
13 BCL6, dilution 1:50; anti-phospho-p70S6K (T389) 1:50; anti-CD79A, dilution 1:100; anti-MUM1,
14 dilution 1:100; anti-c-Myc, dilution 1:100) (see IHC procedure in “GAPDH immunohistochemical
15 (IHC) staining and scoring” section).

16 Tissue-microarrays (TMA) from the LYSA group (validation cohort) were treated and
17 immunoassayed for the same proteins using standard procedures of the LYSA platform as previously
18 described (Molina et al., 2014). GCB vs non-GCB scoring according to the Hans algorithm (Hans et
19 al., 2004), as well as MYC and BCL2 were evaluated (Petrella et al., 2017). In 30 out of the 294 cases,
20 COO classification by IHC (Hans algorithm) could not be assessed. The thresholds employed were
21 40% for MYC and 70% for BCL2 as previously reported (Green et al., 2012; Johnson et al., 2012).

22 FISH analyses were performed on 3µm tissue sections using split signal FISH DNA probes for
23 cMYC/8q24 (Y5410, Dako), BCL2/18q21 (Y5407, Dako), BCL6/3q27 (Y5408, Dako) and slides
24 were analyzed as previously described (Copie-Bergman et al., 2009). Scoring of the hybridization
25 signals were performed according to the algorithm published by (Haralambieva et al., 2002).

26

1 *ATP analysis*

2 ATP was measured using the Cell Titer Glo kit (G7570, Promega). Briefly, 20.000 cells were
3 resuspended in 80 μ L of corresponding medium supplemented with 10% FBS and distributed in a 96
4 well plate. Cells were then treated in triplicates for one hour with PBS (control), or sodium iodoacetate
5 (100 μ M) to inhibit glycolysis, or a combination of 100 μ M of iodoacetate (I9148, Sigma-Aldrich) and
6 10 μ g/ml of oligomycin (O4876, Sigma-Aldrich) to obtain the residual amount of ATP. Short time
7 treatment (1h) was chosen to avoid a metabolic switch upon inhibition of glycolysis and to avoid cell
8 death upon inhibition of both metabolic pathways. 100 μ L of Cell Titer Glo reaction mix was then
9 added to each well for a final volume of 200 μ L. Plates were analyzed for luminescence with a
10 Luminoscan (Berthold Technologies). We verified that ATP measurements were in the linear range of
11 the detection. The difference between total ATP production and the ATP produced under iodoacetate
12 treatment results in glycolytic ATP contribution. Glycolytic ATP is represented by percentage of total
13 ATP produced by the cells.

14

15 *Lactate measurement*

16 Lactate concentration in the supernatant was determined by an enzyme-based assay using 900 μ M β -
17 NAD⁺ (N1636, Sigma-Aldrich), 175 μ g/ml L-lactic dehydrogenase (L2500, Sigma-Aldrich) and 100
18 μ g/ml glutamate-pyruvate transaminase (#10737127001, Roche) diluted in a 620 mM sodium
19 carbonate (S2127, Sigma-Aldrich)-79 mM L-glutamate (G1626, Sigma-Aldrich) buffer adjusted to pH
20 10. Lithium lactate (L2250, Sigma-Aldrich) was used as a standard. Measurements were recorded
21 from a microplate reader (excitation 355 nm, emission 612 nm) after 30 min incubation at 37 °C.
22 Lactate secretion was expressed as mM and normalized to viable cell numbers (using Trypan blue
23 exclusion method).

24

25 Lactate concentration in the supernatant was also determined electro-enzymatically using the YSI
26 2950 Biochemistry Analyzer (Yellow Springs Instruments) and normalized to viable cell number.

1

2 ***Glutamine consumption***

3 Cells were grown in DMEM high glucose, no glutamine (#11960044, Thermo Fisher Scientific)
4 supplemented with 2 mM of L-Glutamine (#25030081, Thermo Fisher Scientific), 10% FBS, 50 μ M
5 of 2-mercaptoethanol (#31350010, Thermo Fisher Scientific), 0.37 mM of L-asparagine (A0884,
6 Sigma-Aldrich) and 10 mM of HEPES pH 7.4 (#15630056, Thermo Fisher Scientific) for 24 hours.
7 The concentrations of L-Glutamine (mg/L) from cultured-cell supernatants were determined electro-
8 enzymatically using the YSI 2950 Biochemistry Analyzer (Yellow Springs Instruments) and
9 normalized to viable cell number.

10

11 ***L-[¹⁴C]-Glutamine uptake***

12 Cells (5×10^6 , in triplicate for each lymphoma) were washed with PBS and incubated 5 min at 37°C in
13 80 μ l of pre-warmed DMEM low glucose (5.5 mM), amino acid-, pyruvic acid- HCO_3^- -free (US
14 Biological, D9800-13) supplemented to a final concentration of 15 mM D-glucose (G6152, Sigma-
15 Aldrich), 20 mM HEPES (#15630056, Thermo Fisher Scientific) and adjusted to pH 7.4, prior
16 addition of 1.25 μ Ci/ml of L-[¹⁴C]-Glutamine (NEC451050UC, PerkinElmer,) for 30 min at 37°C in a
17 CO_2 -free incubator. Subsequently, cells were washed twice with PBS and lysed with 120 μ l of 0.1N
18 NaOH and mixed with 3 ml of Ultima Gold (#6013321, PerkinElmer). Radioactivity was measured
19 using a β -scintillation counter. Inhibition experiments were performed in the presence of 10 mM of the
20 system A transporter inhibitor α -(Methylamino)isobutyric acid (MeAIB, M2383, Sigma-Aldrich).

21

22 ***2-NBDG uptake***

23 200.000 cells were incubated in glucose-free DMEM medium (#11966025, Thermo Fisher Scientific)
24 containing 40 μ M 2-NBDG (#23002-v, Peptide Institute) for 2 hours and analyzed by flow cytometry
25 (Miltenyi Biotec) in the presence of 0.5 μ g/ml of DAPI (D9542, Sigma-Aldrich) to represent glucose
26 uptake (Mean Fluorescence intensity) in viable cells.

1

2 ***Measurement of the mitochondrial mass***

3 The mitochondrial mass was measured by flow cytometry (Miltenyi Biotec) in viable (DAPI negative)
4 cells), after 30 min incubation of cells at 37°C in the presence of 150 nM of Mitotracker green probe
5 (M7514, Invitrogen).

6

7 ***Oxygen consumption***

8 *Polarographic studies:* Intact cell respiration and mitochondrial substrates oxidation on 0.004%
9 digitonin (D5628, Sigma-Aldrich)-permeabilized cells were carried out as previously described
10 (Rustin et al., 1994). Proteins were measured according to Bradford microassay (#500-006, Bio-Rad).
11 Results were expressed in nanomols of oxygen per minute per milligram of proteins or per cell
12 number.

13 *XF Seahorse Analyzer:*

14 Oxygen consumption rate (OCR) was measured in real time using the XF96 extracellular flux analyzer
15 (Agilent). Eμ-Myc cells were seeded on Cell-Tak (#10317081, Thermo Fisher Scientific)- coated
16 XF96 plates at 0.12x10⁶ cells/well in 180 μl of XF base medium minimal DMEM media (#102353-
17 100, Agilent) supplemented with 20 mM D-glucose (G6152, Sigma-Aldrich), 1 mM sodium pyruvate
18 (#11360088, Thermo Fisher Scientific), 2 mM L-glutamine (#25030081, Thermo Fisher Scientific)
19 and adjusted to pH 7.4. The plates were spun at 200 g (breaks off) and incubated at 37°C for 20 min to
20 ensure cell attachment. Measurements were obtained under basal conditions and in response to
21 mitochondrial inhibitors, 1 μM oligomycin (O4876, Sigma-Aldrich), 0.5 μM of Carbonyl cyanide 4-
22 (trifluoromethoxy)phenylhydrazine (FCCP, C2920, Sigma-Aldrich), and 1μM rotenone (R8875,
23 Sigma-Aldrich) combined with 2μM antimycin A (A8674, Sigma-Aldrich).

24

25 ***Mitochondrial respiratory complex activities***

1 Enzymatic spectrophotometric measurements of the OxPhos respiratory chain complex I, complex II
2 and citrate synthase were performed at 37°C on cells according to standard procedures (Rustin et al.,
3 1994). Proteins were measured according to Bradford microassay (#500-006, Bio-Rad). Results are
4 expressed as activity ratios compared to the activity of citrate synthase.

5

6 ***Cell viability assays***

7 Cells (0.3×10^6) were seeded in 96 well-plates in the presence or absence (Ctl, DMSO or NaCl 0.9%)
8 of phenformin (P7045, Sigma-Aldrich), *E-Coli* L-asparaginase (Kidrolase®, Jazz Pharmaceutical),
9 Rapamycin (#1292, Bio-technie) or anti-CD20 antibody Rituximab (Mabthera®, #9197719, Roche) at
10 indicated concentration and period of time. Cells were then labeled with 0.5 µg/ml of DAPI (D9542,
11 Sigma-Aldrich) and analyzed immediately by flow cytometry (Miltenyi Biotec).

12

13 ***Activation of the B-cell receptor***

14 SU-DHL-6 cells (1.10^6 cells/ml) were incubated in the presence of 10 µg/ml of anti-IgM antibody
15 (#109-006-129, Jackson ImmunoResearch) for 10 min and 18hours.

16

17 ***Isolation of human tumor cells from DLBCL core-needle biopsies***

18 ‘Fresh’ image-guided core-needle biopsies (non-frozen tumor biopsies) were harvested in the
19 radiology departments of St Louis hospital in Paris (APHP, France), Centre Hospitalier Princesse
20 Grace (CHPG, Monaco) and the Centre Antoine Lacassagne (CAL, Nice, France), anonymized and
21 immediately sent to our laboratory (Nice, France) in accordance with the GlyPhome protocol
22 approved by institutional review boards of APHP, CHPG and CAL and Commission Nationale de
23 l'Informatique et des Libertés (CNIL) reference 912657 V1. All patients gave written non-opposition
24 consent. Immediately upon receipt, tumor cells were dissociated in RPMI medium (#61870044,
25 Thermo Fisher Scientific) supplemented with 2% of FBS, 10 µg/ml of DNase (D4627, Sigma-
26 Aldrich) and 0.1 mg/ml of collagenase (C9891, Sigma-Aldrich) 5 min at 37°C. Red blood cells were

1 Mm99999915_g1; human *gapdh*: Hs02758991_g1, Thermo Fisher Scientific) on the Step One
2 (Applied Biosystems) according to the manufacturer's instructions. For mouse primary malignant B
3 cells, samples were normalized to mouse *m18s* (Mm03928990_g1, Thermo Fisher Scientific). For
4 human DLBCL cell lines, samples were normalized to human *rplp0* (Hs99999902_m1, Thermo Fisher
5 Scientific).

6 To measure *gapdh* mRNA stability, cells were treated with 5 µg/ml of Actinomycin D (A9415,
7 Sigma-Aldrich) for indicated period of times.

8

9 ***Western blot analysis***

10 Cells were washed in PBS and lysed in laemmli buffer. Tissue samples were collected and lysed in
11 Precellys 24 (Bertin Instruments) homogenizer (3x30 s, 6500g) in laemmli buffer. After quantification
12 (Pierce BCA Protein Assay kit, #23225, Thermo Fisher Scientific), 40 µg of proteins were separated
13 on 8% to 13% SDS polyacrilamide gels and transferred onto polyvinylidene difluoride membranes
14 (Millipore). Membranes were blotted with antibodies against indicated proteins. Immunoreactive
15 bands were detected with an anti-mouse (#7076, Cell Signaling Technology) or an anti-rabbit (7074S,
16 Cell Signaling Technology) IgG horseradish peroxidase (HRP)-linked antibodies. Immunoblots were
17 visualized (FUJIFILM LAS4000) by chemoluminescence using Pierce ECL Western Blotting
18 substrates (#32106, Pierce ECL, Thermo Fisher Scientific). When indicated, Western blot
19 quantification was performed using ImageJ software.

20 Anti-V5 (R96025) was purchased from Invitrogen. Anti-Erk2 (sc-1647) was purchased from Santa
21 Cruz. Anti-GAPDH (ab9485), anti-LDH (ab52488), anti-LDH-B (ab85319), anti-GLS (ab93434) were
22 purchased from Abcam. Anti-HKII (#2106), Anti-ENO1 (#3810), anti-PKM2 (#3198), anti-p53
23 (#2524), anti-phospho-ACC (Ser 79) (#11818), anti-ACC (3676), anti-phospho-p70-S6K (T389)
24 (#9234), anti-p70S6K (#9202), anti-phospho-Syk (Tyr 525/526) (#2710), anti-Syk (#2712) were
25 purchased from Cell Signaling Technology.

26

1 ***Flow cytometry analysis***

2 Intracellular staining for GAPDH was performed using the Cytofix/Cytoperm kit (#554714, BD
3 Biosciences), anti-GAPDH (ab9485, Abcam) and Alexa-Fluor 647 goat anti-rabbit IgG secondary
4 antibody (ab150087, Abcam).

5 IgG and IgM expressions on the surface of DLBCL cell lines were analyzed using FITC-anti-IgG
6 (#130-093-192, Miltenyi Biotec) and APC-anti-IgM (#130-093-076, Miltenyi Biotec).

7 Staining were analyzed by flow cytometry (Miltenyi Biotec). Analysis of the FACS data was
8 performed using Macsquantify Version 2.11 (Miltenyi).

9

10 ***Targeted LC-MS metabolites analyses***

11 Metabolites were extracted as described (Mackay et al., 2015). Briefly, 1.10^6 E μ -Myc cells (4
12 replicates per clones) were used for extraction. Extraction solution was composed of 50% methanol,
13 30% ACN, and 20% water. The volume of extraction solution added was adjusted to the number of
14 cells (0.5 ml/ 1×10^6 cells). After addition of extraction solution, samples were vortexed for 5 min at
15 4°C and then centrifuged at 16,000 g for 15 min at 4°C. The supernatants were collected and stored at
16 -80°C until analyses. Liquid chromatography/Mass Spectrometry (LC/MS) analyses were conducted
17 on a QExactive Plus Orbitrap mass spectrometer equipped with an Ion Max source and a HESI II
18 probe and coupled to a Dionex UltiMate 3000 UPLC system (Thermo, USA). External mass
19 calibration was performed using the standard calibration mixture every 7 days as recommended by the
20 manufacturer. 5 μ l of each sample was injected onto Zic-pHilic (150 mm \times 2.1 mm i.d. 5 μ m) with the
21 guard column (20 mm \times 2.1 mm i.d. 5 μ m) (Millipore) for the liquid chromatography separation.
22 Buffer A was 20 mM ammonium carbonate, 0.1% ammonium hydroxide (pH 9.2); buffer B was
23 acetonitrile. The chromatographic gradient was run at a flow rate of 0.200 μ l/min as follows: 0–
24 20 min; linear gradient from 80% to 20% B; 20–20.5 min; linear gradient from 20% to 80% B; 20.5–
25 28 min: hold at 80% B (Mackay et al., 2015). The mass spectrometer was operated in full scan,
26 polarity switching mode with the spray voltage set to 2.5 kV, the heated capillary held at 320°C. The

1 sheath gas flow was set to 20 units, the auxiliary gas flow was set to 5 units, and the sweep gas flow
2 was set to 0 unit. The metabolites were detected across a mass range of 75–1,000 m/z at a resolution of
3 35,000 (at 200 m/z) with the AGC target at 106, and the maximum injection time at 250 ms. Lock
4 masses were used to insure mass accuracy below 5 ppm. Data were acquired with Thermo Xcalibur
5 software (Thermo Fisher Scientific). The peak area of metabolites was determined using Thermo
6 TraceFinder software (Thermo Fisher Scientific), identified by the exact mass of each singly charged
7 ion and by known retention time on the HPLC column. Statistical analyses were performed using
8 Metaboanalyst 4.0 software.

9

10 *¹H HRMAS NMR spectroscopy*

11 Cell pellets (10 million cells) were frozen at -80°C. After thawing cell pellets, 10 microliters of D₂O
12 were added. Solvent and cells were then placed into a 30 µl disposable insert introduced into a 4mm
13 ZrO₂ HRMAS rotor before NMR analysis. All the NMR experiments were recorded on a Bruker
14 Avance III spectrometer operating at 400 MHz and 100MHz for ¹H and ¹³C, respectively, and
15 equipped with a ¹H/¹³C/³¹P HRMAS probe. All the spectra were recorded at 4000 Hz spinning rate and
16 a temperature of 277 K. For each sample, ¹H HRMAS NMR spectrum was acquired using the Carr-
17 Purcell-Meiboom-Gill NMR sequence, preceded by a water presaturation pulse during relaxation time
18 of 2 s. This sequence enables us to reduce the macromolecule and lipid signal intensities using a T2
19 filter of 50 ms synchronised with the rotor rotation speed. For each spectrum, 256 free induction
20 decays of 20 800 data points, were collected using 8000 Hz of spectral window. The FIDs were
21 multiplied by an exponential weighting function corresponding to a line broadening of 0.3 Hz and
22 zero-filled prior to Fourier transformation. The calibration on the alanine doublet (δ=1.47 ppm) and
23 the phase and baseline corrections were performed manually for all the spectra. The identification of
24 the NMR signals was carried out using ¹H-¹H TOCSY, ¹H-¹³C HSQC NMR experiments, online
25 databases (HMDB, BRMB) and literature (Nicholson et al., 1995; Wishart et al., 2013). Each
26 spectrum was divided into 0.005 ppm-width integrated buckets and normalized to total spectrum
27 intensity after having removed the presaturated water signal region (4.85 -5.10 ppm) using AMIX

1 software (Bruker Biospin GmbH, Karlsruhe, Germany). The water region must be removed due to
2 inconsistent signal suppression.

3 A matrix of 42 samples and 1700 buckets was then created and exported to the software Simca-P v13
4 (Umetrics, Umea, Sweden) for statistical analysis. Principal component analysis was first performed in
5 order to detect intrinsic clusters and outliers within the dataset. Since expected discrimination was not
6 achieved using PCA, the data were analyzed with orthogonalized projections to latent structures
7 discriminant analysis (OPLS-DA). The OPLS algorithm derives from basic partial least-squares (PLS)
8 regression and allows a more effective use of the relevant discriminating variables by removing
9 information orthogonal to the Y matrix (matrix containing the sample classes), i.e., not relevant for
10 this particular discrimination. The resulting scores and loading plots were used to visualize
11 respectively the samples and the NMR frequency signals (variables) in the predictive and orthogonal
12 reduced component frame. Resampling the model 999 times under the null hypothesis performed
13 OPLS-DA model validation, i.e. by generating 999 models for each between 50 to 100 % of the Y
14 matrix were permuted. The quality of the model was assessed by monitoring changes in goodness-
15 of-fit and predictive statistics, R²_Y and Q², respectively, between the models calculated from the
16 permuted Y-matrix and the original one.

17 The normalized signals of each discriminant metabolite were then integrated for each spectrum in
18 order to calculate their respective fold change between the two groups. The significance of the fold
19 change was tested using a two-tailed t-test with a significance level of 0.05.

20

21 Plasma samples (200 µl) were frozen at -80 C. After thawing, 400 µl of 0.9% saline solution in
22 D₂O was added. Samples were then placed into a 5mm NMR tube and NMR experiments were
23 recorded on a Bruker Avance III spectrometer operating at 600 MHz and 150MHz for ¹H and ¹³C,
24 respectively, and equipped with a ¹H/¹³C TXI probe. Spectra were recorded at 300 K. A Carr-Purcell-
25 Meiboom-Gill (CPMG) NMR spin echo sequence [90° — (τ — 180° — τ)_n] with an effective spin
26 echo time of 75.6 ms, preceded by a water presaturation pulse during the relaxation time was
27 employed to reduce the signal intensities of lipids and macromolecules. A relaxation time of 33 s was

1 necessary to achieve full relaxation for all the metabolites in order to enable absolute quantification.
2 For each sample, 128 free induction decays (FID) of 32768 complex data points were collected using a
3 spectral width of 12 000 Hz. A sample of 1.67 mM of maleic acid was used as an external reference to
4 calibrate the ERETIC signal (electronic signal) used for the quantification of glutamine.

5

6 **Quantification and Statistical Analysis**

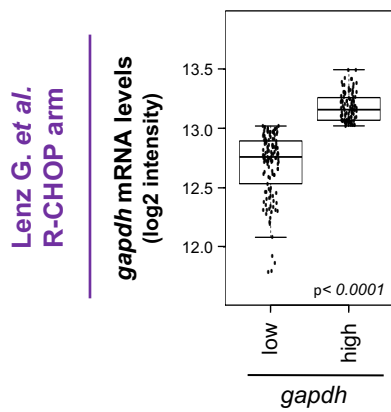
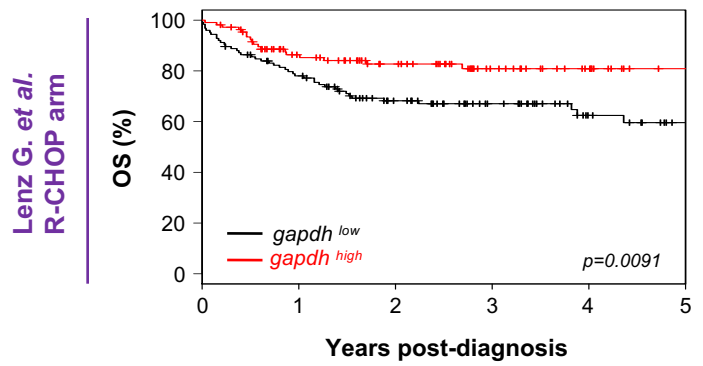
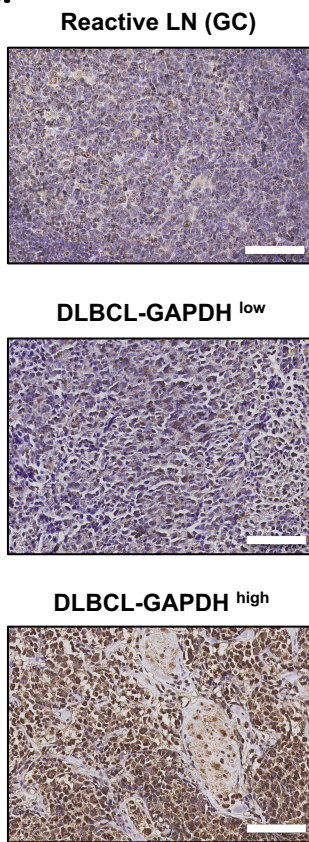
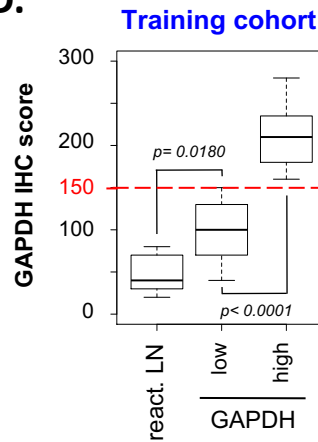
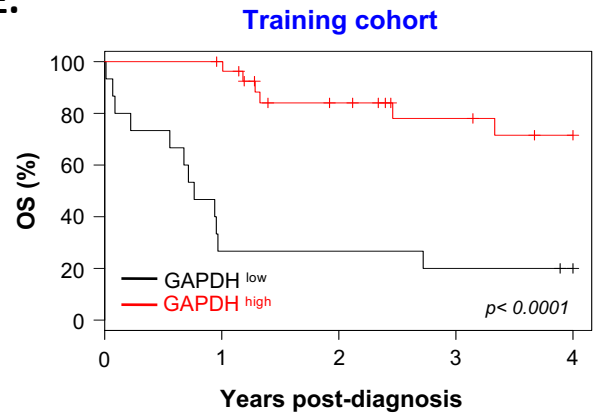
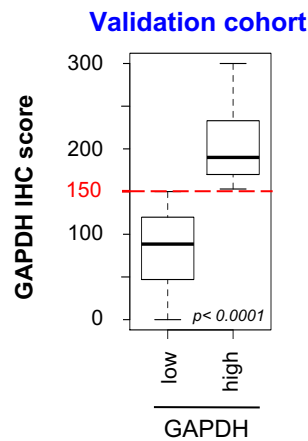
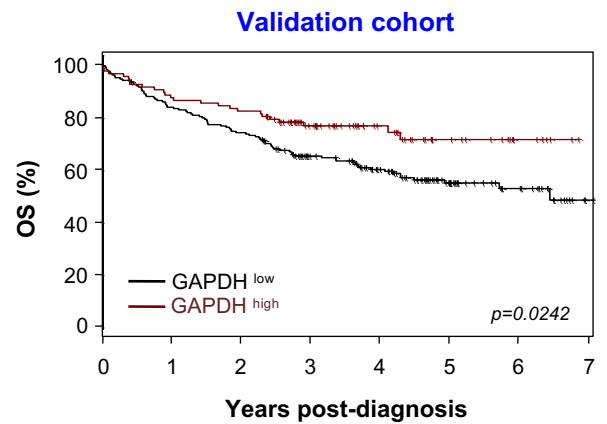
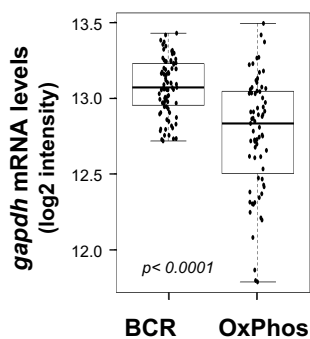
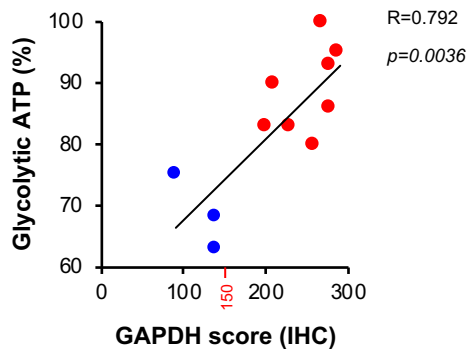
7 All survival analyses were performed on an intention-to-treat basis. Categorical variables were
8 compared using the chi-squared or Fisher exact tests. Progression-free survival (PFS) was defined as
9 the time from study entry until disease progression or death. Overall survival (OS) was defined as the
10 time from the start of treatment until death. Survival functions were estimated using the Kaplan-Meier
11 method and compared with the log-rank test. Comparative tests were considered significant if a 2-
12 sided $p < 0.05$. Because the LNH2003-6 trial was not stratified by biological data, we controlled for the
13 effects of prognostic factors on outcome due to sampling fluctuations in the treatment groups with a
14 multivariate analysis of survival in a Cox model. Statistical analyses of clinical data were performed
15 using R project software or SAS 9.2 (SAS Institute) and S-Plus 6.2 (MathSoft) software. Data
16 distributions are presented using boxplots when needed, to provide a graphical representation of the
17 variance. Statistical significance was assessed using the Wilcoxon rank sum test. For all other clinical
18 data, statistical analyses used for each of the figures is specified in the legends. For *in vitro*
19 experiments, results are expressed as mean (-/+ s.d.) and statistical analyses were performed using
20 two-tailed Student's t-test. A p value of less than 0.05 was considered to indicate statistical
21 significance (* $p < 0.05$, ** $p < 0.01$ and *** $p < 0.001$). n for the different groups are provided in the
22 figure legends.

23

24 **Data analysis and Software availability**

25 ***Code availability***

26 R code for microarray analysis of Lenz G. et al. data set is available at [doi:10.17632/f4f3wbszmd.1](https://doi.org/10.17632/f4f3wbszmd.1)

A.**B.****C.****D.****E.****F.****G.****H.****I.****Figure 1 Chiche J et al.**

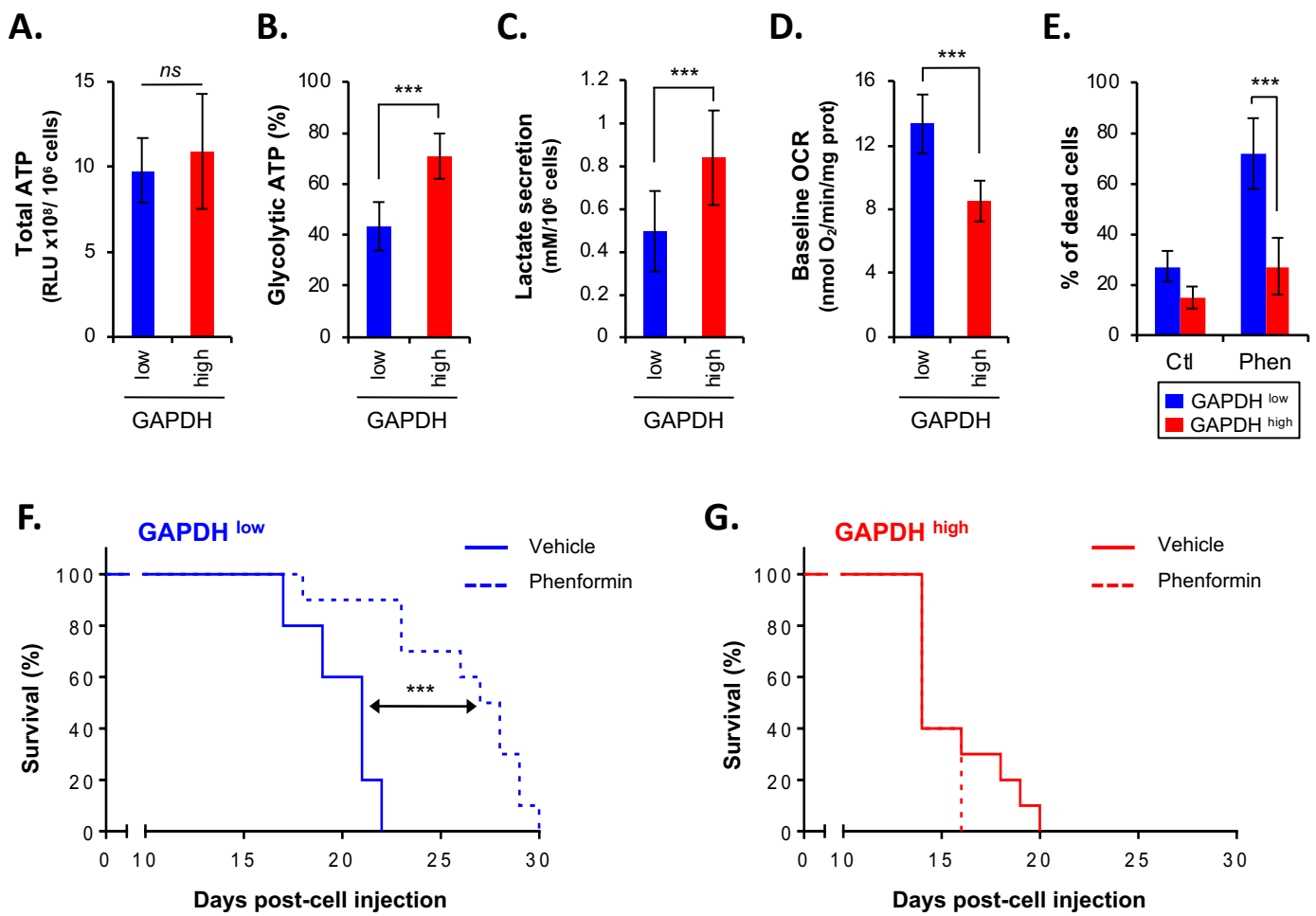


Figure 2 Chiche J et al.

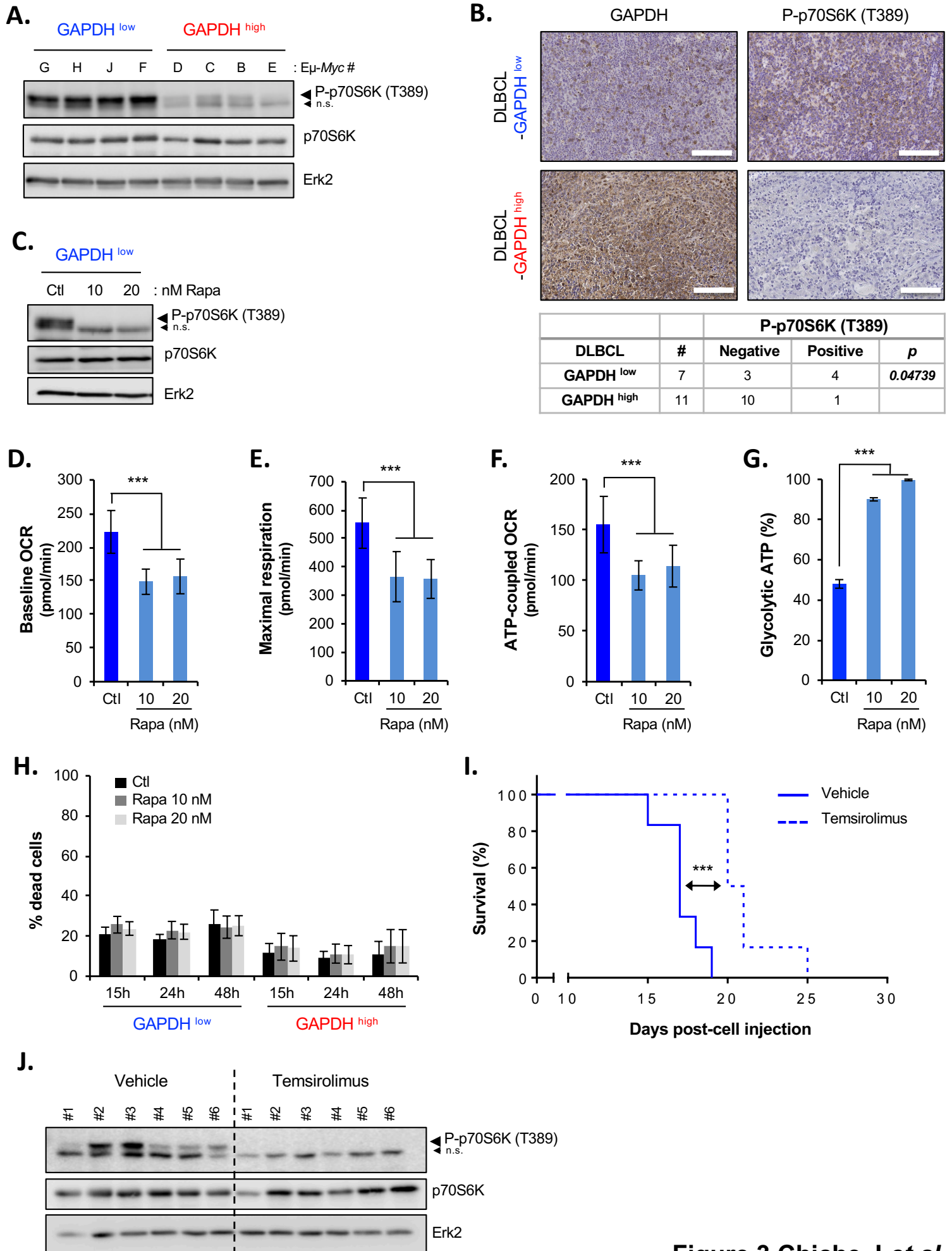


Figure 3 Chiche J et al.

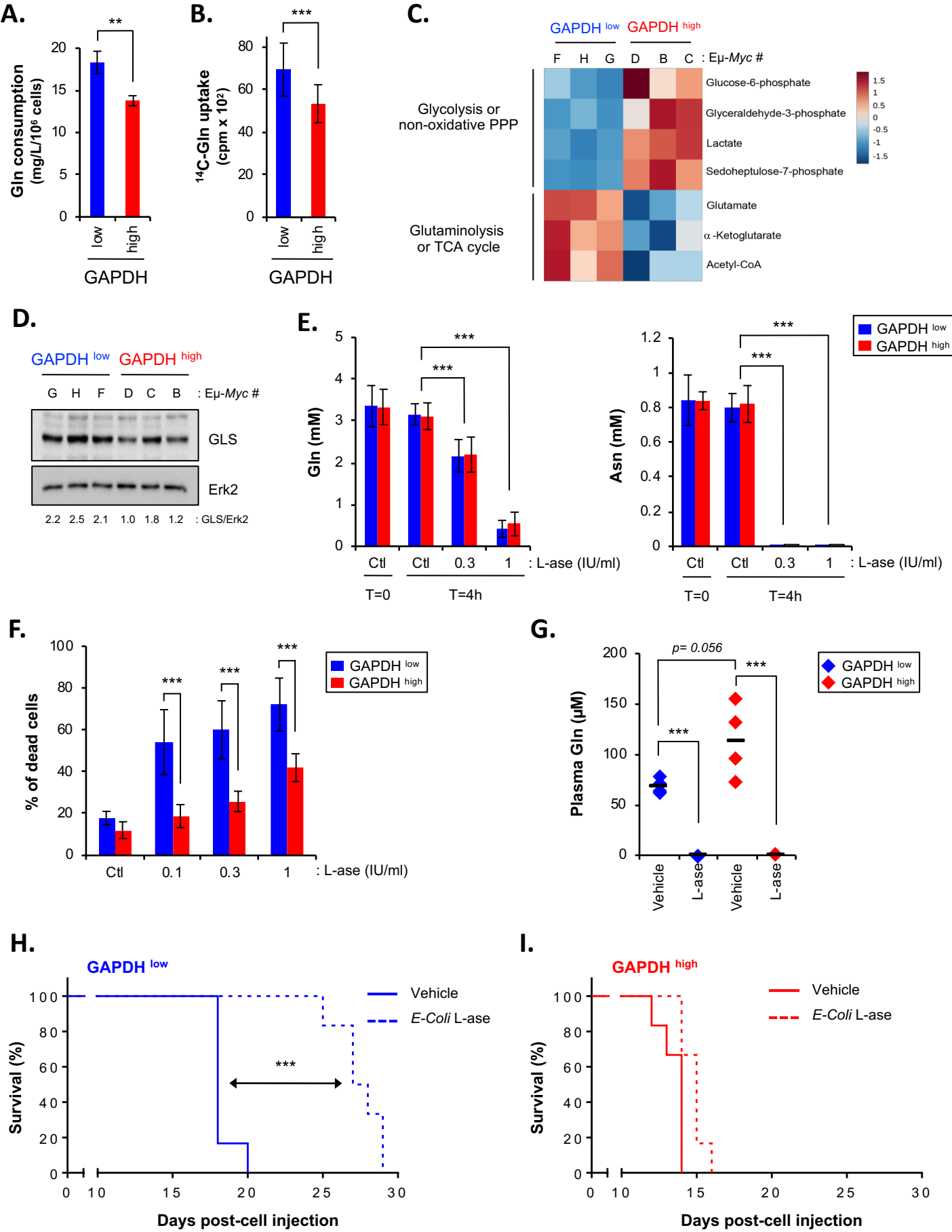


Figure 4 Chiche J et al.

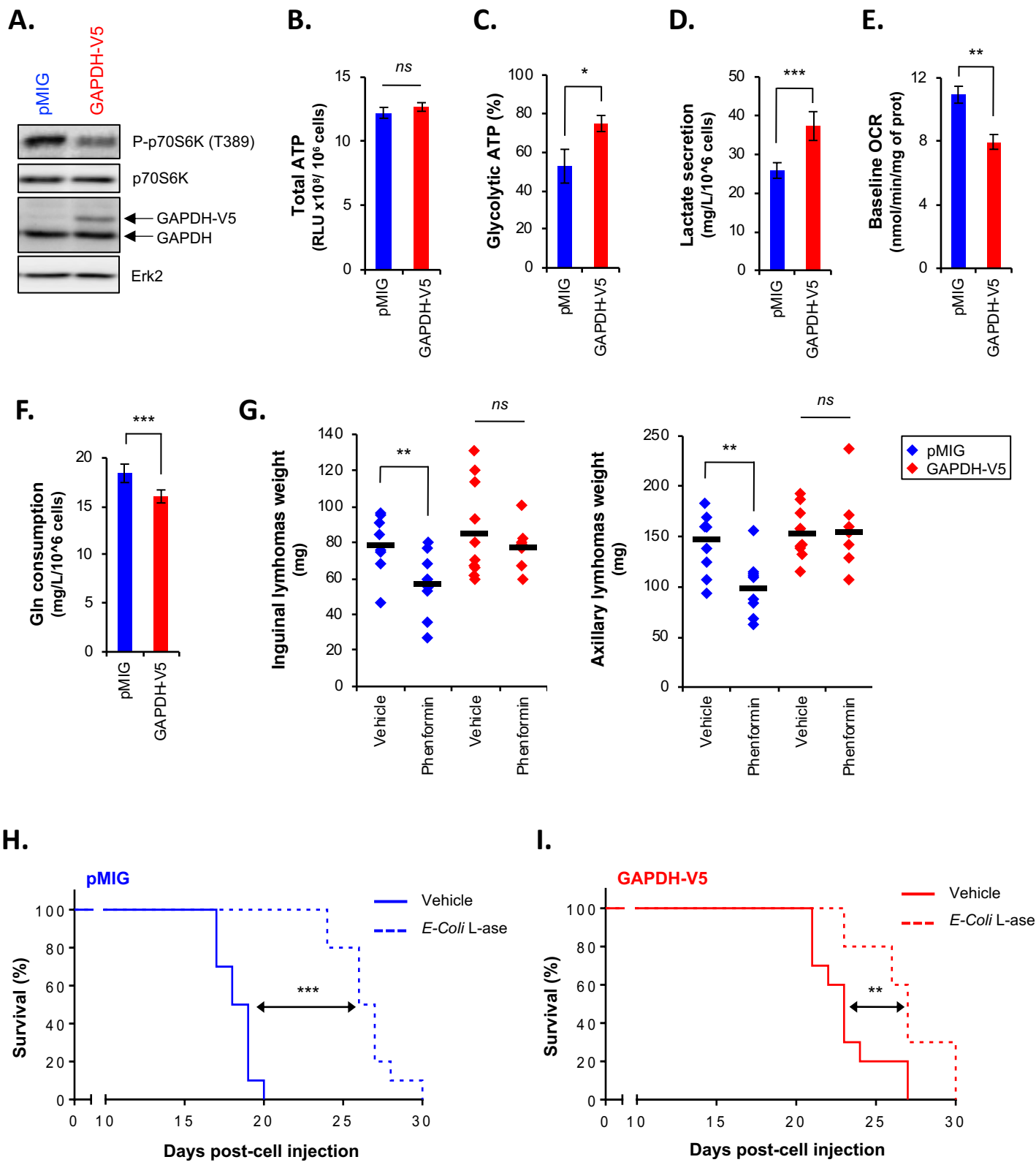
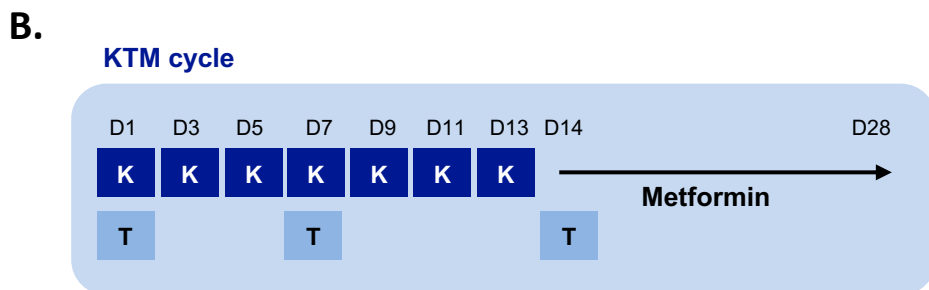
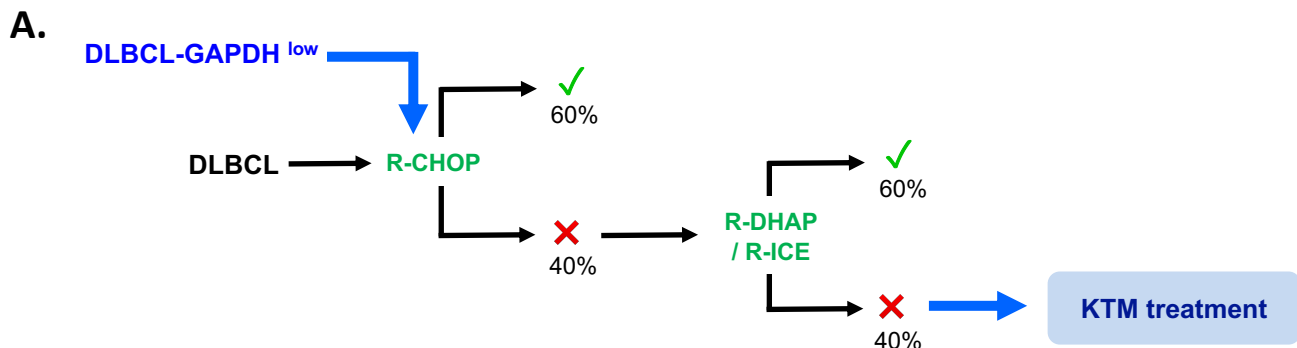
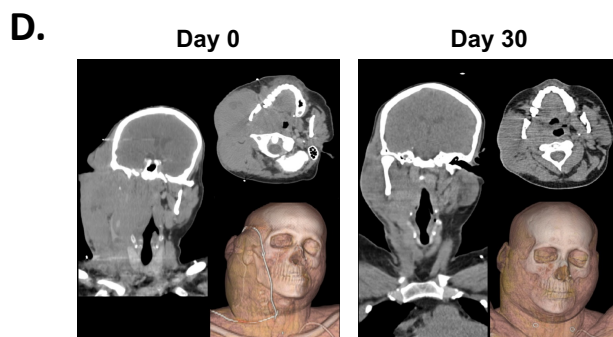


Figure 5 Chiche J et al.



Patient #1- DLBCL-*Myc*⁺/GAPDH^{low}
Refractory to R-based therapies



Patient #1

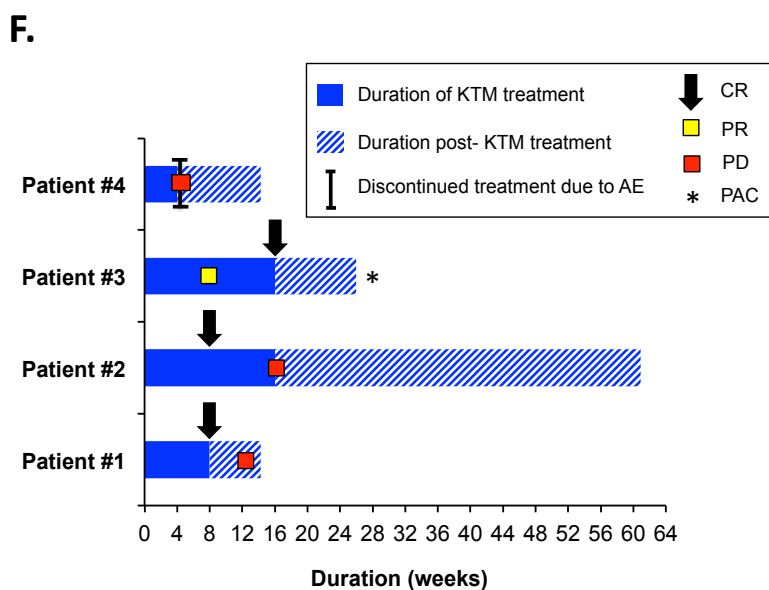
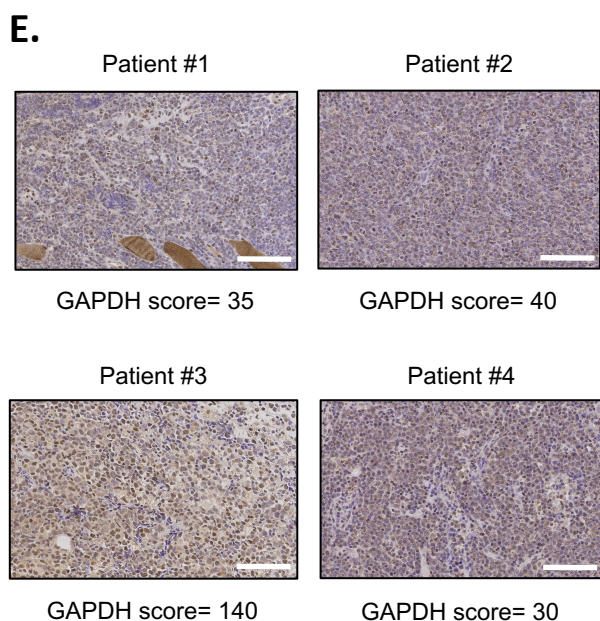


Figure 6 Chiche J *et al.*

Table 1. GAPDH expression levels are not associated with other biological prognostic factors.

DLBCL		TRAINING COHORT (n=43)				<i>p</i>	VALIDATION COHORT (n=294)				<i>p</i>
		GAPDH ^{low} (n=15)		GAPDH ^{high} (n=28)			GAPDH ^{low} (n=204)		GAPDH ^{high} (n=90)		
		No.	%	No.	%		No.	%	No.	%	
PARAMETERS											
Bcl2	< 70%	1	6.7	10	35.7	0.0648	66 (a)	37.7	35 (b)	40.2	0.7876
	≥ 70%	14	93.3	18	64.3		109 (a)	62.3	52 (b)	59.8	
Bcl6	≤ 25%	6	40	18	64.3	0.1982	63 (c)	36.2	33 (d)	39.3	0.6808
	> 25%	9	60	10	35.7		111 (c)	63.8	51 (d)	60.7	
Myc	< 40%	5	33.3	23 (e)	85.2	0.0014	98 (f)	62.4	48 (g)	72.7	0.1657
	≥ 40%	10	66.7	4 (e)	14.8		59 (f)	37.6	18 (g)	27.3	
DE (Myc-Bcl2)	Myc < 40% ; Bcl2 < 70%	6	40	26 (e)	85.2	9.38 e-05	115 (h)	73.3	51 (i)	78.5	0.4990
	Myc ≥ 40% ; Bcl2 ≥ 70%	9	60	1 (e)	14.8		41 (h)	26.3	14 (i)	21.5	
Double Hit Myc/Bcl2	No	4 (j)	100	11 (k)	91.67	1.0000	148 (l)	92.5	60 (m)	95.2	0.5652
	Yes	0 (j)	0	1 (k)	8.33		12 (l)	7.5	3 (m)	4.8	
Triple Hit Myc/Bcl2/Bcl6	No	4 (j)	100	12 (k)	100	n.a	158 (l)	98.7	62 (m)	98.4	1.0000
	Yes	0 (j)	0	0 (k)	0		2 (l)	1.3	1 (m)	1.6	

Abbreviations: DE, double expressors (Myc-Bcl2); GAPDH, glyceraldehyde-3-phosphate dehydrogenase; R-CHOP, Rituximab with cyclophosphamide, doxorubicin, oncovin and prednisone.

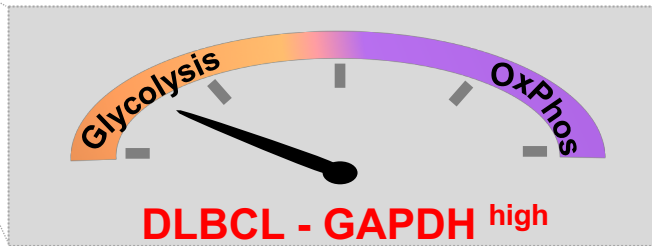
n.a, not applicable.

Number of samples that could not be analyzed: (a) 29; (b) 3; (c) 30; (d) 6; (e) 1; (f) 47; (g) 24; (h) 48; (i) 25; (j) 11; (k) 16; (l) 44; (m) 27.

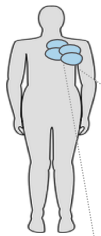
DLBCL GAPDH High



R-CHOP



DLBCL GAPDH Low



R-CHOP



KTM

